



**NAVAL  
POSTGRADUATE  
SCHOOL**

**MONTEREY, CALIFORNIA**

**THESIS**

**EVALUATION OF CONVECTIVE WIND FORECASTING  
METHODS DURING HIGH WIND EVENTS**

by

Christopher J Kuhlman

March 2006

Thesis Advisor:  
Second Reader:

Wendell A. Nuss  
Carlyle H. Wash

**Approved for public release; distribution is unlimited.**

THIS PAGE INTENTIONALLY LEFT BLANK

REPORT DOCUMENTATION PAGE			Form Approved OMB No. 0704-0188	
Public reporting burden for this collection of information is estimated to average 1 hour per response, including the time for reviewing instruction, searching existing data sources, gathering and maintaining the data needed, and completing and reviewing the collection of information. Send comments regarding this burden estimate or any other aspect of this collection of information, including suggestions for reducing this burden, to Washington headquarters Services, Directorate for Information Operations and Reports, 1215 Jefferson Davis Highway, Suite 1204, Arlington, VA 22202-4302, and to the Office of Management and Budget, Paperwork Reduction Project (0704-0188) Washington DC 20503.				
1. AGENCY USE ONLY (Leave blank)		2. REPORT DATE March 2006	3. REPORT TYPE AND DATES COVERED Master's Thesis	
4. TITLE AND SUBTITLE: Evaluation of Convective Wind Forecasting Methods During High Wind Events			5. FUNDING NUMBERS	
6. AUTHOR(S) Christopher J. Kuhlman				
7. PERFORMING ORGANIZATION NAME(S) AND ADDRESS(ES) Naval Postgraduate School Monterey, CA 93943-5000			8. PERFORMING ORGANIZATION REPORT NUMBER	
9. SPONSORING /MONITORING AGENCY NAME(S) AND ADDRESS(ES) N/A			10. SPONSORING/MONITORING AGENCY REPORT NUMBER	
11. SUPPLEMENTARY NOTES The views expressed in this thesis are those of the author and do not reflect the official policy or position of the Department of Defense or the U.S. Government.				
12a. DISTRIBUTION / AVAILABILITY STATEMENT Approved for public release; distribution is unlimited			12b. DISTRIBUTION CODE	
13. ABSTRACT (maximum 200 words) This study investigates convective wind gust forecasting methods for reported gusts in the Midwest, Central, and Northeast United States from June and July 2005. Three methods are examined using MM5 model data; the T <sub>1</sub> and T <sub>2</sub> methods and the WINDEX method. The model-derived wind gusts determined by each method are then compared to wind reports from the Storm Prediction Center's severe storm reports archive and reports from observing stations. Model-derived wind gusts are then compared to the observed wind gusts for varying times of day and observed wind gust ranges. Wind gust frequency plots are examined for each wind method to determine accuracy and to characterize any patterns. The T <sub>1</sub> method was the most accurate overall for this study, but was shown to be less sensitive to varying atmospheric conditions. The T <sub>2</sub> method was the least accurate of the three methods during all situations. The WINDEX method performed well in most situations and was nearly as accurate as the T <sub>1</sub> method, while WINDEX also proved to be the most sensitive of the three to varying mesoscale conditions.				
14. SUBJECT TERMS Convective Wind Forecasting Methods, Model-derived Wind Gusts, T <sub>1</sub> Method, T <sub>2</sub> Method, WINDEX Method			15. NUMBER OF PAGES 81	
			16. PRICE CODE	
17. SECURITY CLASSIFICATION OF REPORT Unclassified	18. SECURITY CLASSIFICATION OF THIS PAGE Unclassified	19. SECURITY CLASSIFICATION OF ABSTRACT Unclassified	20. LIMITATION OF ABSTRACT UL	

NSN 7540-01-280-5500

Standard Form 298 (Rev. 2-89)  
Prescribed by ANSI Std. Z39-18

THIS PAGE INTENTIONALLY LEFT BLANK

**Approved for public release; distribution is unlimited**

**EVALUATION OF CONVECTIVE WIND FORECASTING METHODS DURING  
HIGH WIND EVENTS**

Christopher J. Kuhlman  
Captain, United States Air Force  
B.S., Valparaiso University, 2001

Submitted in partial fulfillment of the  
requirements for the degree of

**MASTER OF SCIENCE IN METEOROLOGY**

from the

**NAVAL POSTGRADUATE SCHOOL  
March 2006**

Author: Christopher J. Kuhlman

Approved by: Wendell A. Nuss  
Thesis Advisor

Carlyle H. Wash  
Second Reader

Philip A. Durkee  
Chairman, Department of Meteorology

THIS PAGE INTENTIONALLY LEFT BLANK

## ABSTRACT

This study investigates convective wind gust forecasting methods for reported gusts in the Midwest, Central, and Northeast United States from June and July 2005. Three methods are examined using MM5 model data; the  $T_1$  and  $T_2$  methods and the WINDEX method. The model-derived wind gusts determined by each method are then compared to wind reports from the Storm Prediction Center's severe storm reports archive and reports from observing stations. Model-derived wind gusts are then compared to the observed wind gusts for varying times of day and observed wind gust ranges. Wind gust frequency plots are examined for each wind method to determine accuracy and to characterize any patterns. The  $T_1$  method was the most accurate overall for this study, but was shown to be less sensitive to varying atmospheric conditions. The  $T_2$  method was the least accurate of the three methods during all situations. The WINDEX method performed well in most situations and was nearly as accurate as the  $T_1$  method, while WINDEX also proved to be the most sensitive of the three to varying mesoscale conditions.

THIS PAGE INTENTIONALLY LEFT BLANK



# TABLE OF CONTENTS

I.	INTRODUCTION.....	1
A.	<b>THEESIS OBJECTIVES AND MILITARY SIGNIFICANCE.....</b>	<b>1</b>
B.	<b>CONVECTIVELY DRIVEN HIGH WINDS .....</b>	<b>3</b>
1.	Climatology of Damaging Wind Events .....	3
2.	Understanding the Downdraft .....	6
3.	Types of Downdrafts .....	8
II.	TECHNIQUE.....	13
A.	<b>OVERVIEW OF CONVECTIVE WIND FORECASTING METHODS..</b>	<b>13</b>
1.	T <sub>1</sub> Gust Method .....	13
2.	T <sub>2</sub> Gust Method .....	14
3.	WINDEX Gust Method .....	16
III.	DATA AND METHODS.....	17
A.	DATA USED .....	17
1.	Storm Reports.....	17
2.	Model Data.....	19
B.	DATA PROCESSING.....	20
1.	Method Calculations.....	20
2.	Upper Air Soundings .....	21
3.	Visual Program .....	24
IV.	DATA ANALYSIS .....	27
A.	OVERALL RESULTS.....	27
1.	T <sub>1</sub> Gust Method .....	27
2.	T <sub>2</sub> Gust Method .....	33
3.	WINDEX Gust Method .....	39
B.	DIURNAL EFFECTS .....	44
1.	T <sub>1</sub> Gust Method .....	44
2.	T <sub>2</sub> Gust Method .....	46
3.	WINDEX Gust Method .....	48
C.	REPORTS OF UNKNOWN WIND SPEED .....	50
D.	WIND METHOD COMPARISON.....	54
E.	DISCUSSION OF RESULTS .....	56
V.	CONCLUSIONS AND RECOMMENDATIONS.....	59
A.	CONCLUSIONS.....	59
B.	RECOMMENDATIONS.....	59
	LIST OF REFERENCES.....	61
	INITIAL DISTRIBUTION LIST .....	63

THIS PAGE INTENTIONALLY LEFT BLANK

## LIST OF FIGURES

Figure 1.1.	Area of responsibility (AOR) for the 15th Operational Weather Squadron (OWS). The 15th OWS is responsible for 190 different military units including 13 active duty locations within its AOR.....	1
Figure 1.2.	Monthly distribution of occurrences of thunderstorms related wind damaged (light gray) gusts between 25.8 and 33.5 m s-1 (gray) and gusts greater than 33.5 m s-1 (black) (After Kelly et al. 1985).....	4
Figure 1.3.	Hourly distribution in NST of occurrences of thunderstorm related wind damage (stippled) gusts between 25.8 and 33.5 m s-1 (upper left to lower right hatching) and gusts greater than 33.5 m s-1 (cross hatching) (From Kelly et al. 1985).....	5
Figure 1.4.	Dashed black lines are isopleths of one. Values greater than 11 and 17 are shaded gray and black, respectively (After Kelly et al. 1985). .....	5
Figure 1.5.	Schematic cross section through the gust front of a thunderstorm (After Wakimoto 2001).....	9
Figure 1.6.	Schematic view of the supercell thunderstorm at the surface. The gray shading encompasses the radar echo. The gust front structure is depicted using a solid line and frontal symbols. Surface position of the updraft is hatched while the forward-flank downdraft (FFD) and rear-flank downdraft (RFD) are crosshatched (From Wakimoto 2001). .....	10
Figure 1.7.	Conceptual model of a microburst hypothesized to explain ground damage patterns. Three stages of development are shown. A midair microburst may or may not descend to the surface. If it does, the outburst winds develop immediately after reaching the surface (From Wakimoto 2001). .....	11
Figure 1.8.	A typical evolution of radar echoes associated with bow echoes that produce strong and extensive downbursts (From Wakimoto 2001). .....	11
Figure 2.1.	Given a calculated T2 value, wind gust potential can be estimated using the curves (After Miller 1972).....	15
Figure 3.1.	Sample SPC storm report map from 08 June 2005 (From Ref. Storm Prediction Center Severe Weather Events Archive, <a href="http://www.spc.noaa.gov/climo/">http://www.spc.noaa.gov/climo/</a> , February 2006).....	17
Figure 3.2.	Sample of NEXRAD imagery from 08 June 2005 at 22Z (From Ref. National Climatic Data Center, <a href="http://www4.ncdc.noaa.gov/cgi-win/wwcgi.dll?WWNEXRAD~Images2">http://www4.ncdc.noaa.gov/cgi-win/wwcgi.dll?WWNEXRAD~Images2</a> , February 2006).....	19
Figure 3.3.	Observed atmospheric sounding from 00Z. Pressure in millibars on the left and temperature in degrees Celsius on the bottom .....	23
Figure 3.4.	MM5 06Z model run sounding valid at 00Z. Pressure in millibars on the left and temperature in degrees Celsius on the bottom .....	24

Figure 3.5.	Example of computed WINDEX gusts with dark blue colors representing low wind gusts and dark green colors representing high wind gusts. Contour intervals every 10 knots .....	25
Figure 4.1.	Computed T1 gust value versus observed wind gusts for June and July of 2005. ....	28
Figure 4.2.	For observed reports between 35-44 knots: Computed T1 wind gusts are compared to the frequency of times computed it was computed within the range of observed gusts. ....	29
Figure 4.3.	For observed reports between 45-54 knots: Computed T1 wind gusts are compared to the frequency of times computed it was computed within the range of observed gusts. ....	30
Figure 4.4.	For observed reports between 55-64 knots: Computed T1 wind gusts are compared to the frequency of times it was computed within the range of observed gusts. ....	31
Figure 4.5.	For observed reports between 65-74 knots: Computed T1 wind gusts are compared to the frequency of times it was computed within the range of observed gusts. ....	32
Figure 4.6.	Computed T2 gust value versus observed wind gusts for June and July of 2005. ....	34
Figure 4.7.	For observed reports between 35-44 knots: Computed T2 wind gusts are compared to the frequency of times it was computed within the range of observed gusts. ....	35
Figure 4.8.	For observed reports between 45-54 knots: Computed T2 wind gusts are compared to the frequency of times it was computed within the range of observed gusts. ....	36
Figure 4.9.	For observed reports between 55-64 knots: Computed T2 wind gusts are compared to the frequency of times it was computed within the range of observed gusts. ....	37
Figure 4.10.	For observed reports between 65-74 knots: Computed T2 wind gusts are compared to the frequency of times it was computed within the range of observed gusts. ....	38
Figure 4.11.	Computed WINDEX gust value versus observed wind gusts for June and July of 2005. ....	39
Figure 4.12.	For observed reports between 35-44 knots: Computed WINDEX wind gusts are compared to the frequency of times it was computed within the range of observed gusts. ....	40
Figure 4.13.	For observed reports between 45-54 knots: Computed WINDEX wind gusts are compared to the frequency of times it was computed within the range of observed gusts. ....	41
Figure 4.14.	For observed reports between 55-64 knots: Computed WINDEX wind gusts are compared to the frequency of times it was computed within the range of observed gusts. ....	42
Figure 4.15.	For observed reports between 65-74 knots: Computed WINDEX wind gusts are compared to the frequency of times it was computed within the range of observed gusts. ....	43

Figure 4.16. Computed $T_1$ gust value versus observed wind gusts for 21Z events during June 2005. ....	45
Figure 4.17. Computed $T_1$ gust value versus observed wind gusts for 06Z events during June 2005. ....	45
Figure 4.18. Computed $T_2$ gust value versus observed wind gusts for 21Z events during June 2005. ....	46
Figure 4.19. Computed $T_2$ gust value versus observed wind gusts for 06Z events during June 2005. ....	47
Figure 4.20. Computed WINDEX gust value versus observed wind gusts for 21Z events during June 2005. ....	49
Figure 4.21. Computed WINDEX gust value versus observed wind gusts for 06Z events during June 2005. ....	49
Figure 4.22. For unknown wind gusts: Computed $T_1$ wind gusts are compared to the frequency of times it was computed. ....	51
Figure 4.23. For unknown wind gusts: Computed $T_2$ wind gusts are compared to the frequency of times it was computed. ....	52
Figure 4.24. For unknown wind gusts: Computed WINDEX wind gusts are compared to the frequency of times it was computed. ....	53

THIS PAGE INTENTIONALLY LEFT BLANK

## LIST OF TABLES

Table 2.1.	T1 convective gust potential (After Miller 1972).....	14
Table 3.1.	Example of storms reports from SPC from 08 June 2005 (After Ref. Storm Prediction Center Severe Weather Events Archive, <a href="http://www.spc.noaa.gov/climo/">http://www.spc.noaa.gov/climo/</a> , February 2006).....	18
Table 4.1.	Percentage difference between the method computed wind gusts and observed gusts for each three hour time frame for June 2005. ...	55
Table 4.2.	Percentage difference between the method computed wind gusts and observed gusts for each three hour time frame for July 2005.....	55
Table 4.3.	Computed forecast mean values in knots for each method for given observed gust ranges .....	56
Table 4.4.	One standard deviation values in knots for each method for given observed gust ranges .....	56

THIS PAGE INTENTIONALLY LEFT BLANK



## **ACKNOWLEDGMENTS**

I would like to thank my advisor, Professor Wendell A. Nuss of the Department of Meteorology, Naval Postgraduate School, for his guidance and expertise during the development of this thesis. His vast meteorological expertise and programming skills were an integral part in analyzing and processing the data required for this study. Additionally, I would like to thank Professor Carlyle H Wash, Department of Meteorology, Naval Postgraduate School, for his encouragement and assistance as the second reader of this thesis.

I would also like to thank Mr. Robert Creasy, staff meteorologist, Naval Postgraduate School. He provided many hours of computer support, as well as finding the model data used in this study. His help made the data gathering process possible. Finally, I would like to thank Ms. Allison Wreath of the 15<sup>th</sup> Operational Weather Squadron, Scott Air Force Base, Illinois, who served as the point of contact from the agency that initiated this thesis topic.

THIS PAGE INTENTIONALLY LEFT BLANK

# I. INTRODUCTION

## A. THESIS OBJECTIVES AND MILITARY SIGNIFICANCE

Damaging winds can have a great impact on the United States military's assets and personnel from structural damage to buildings and planes to the loss of man-hours. The importance of accurate forecasts of strong to severe thunderstorm wind gusts is vital to the protection of current and future military operations.

The 15<sup>th</sup> Operational Weather Squadron (OWS) at Scott Air Force Base, Illinois proposed a research topic to address current convective wind forecasting methods used by forecasters within the squadron. The 15<sup>th</sup> OWS, one of four Air Force OWS units within the United States, is responsible for providing weather support for an area from the Central and Northern Plains through the Great Lakes into New England (see Figure 1.1). During the summer, this region experiences extensive thunderstorm activity sometimes producing strong to severe wind gusts.



**Figure 1.1.** Area of responsibility (AOR) for the 15th Operational Weather Squadron (OWS). The 15th OWS is responsible for 190 different military units including 13 active duty locations within its AOR.

Within this region, the 15<sup>th</sup> OWS provides convective wind warnings for 190 active duty military, Air National Guard, Air Force Reserve, and Department of Defense installations. Due to the vast area of responsibility and importance of providing convective wind warnings, the need for an accurate method of forecasting thunderstorm wind gusts is vital to the safety of military personnel and resource protection.

The ultimate goal of this thesis is to provide insight into any discrepancies of the current convective wind forecasting methods used by the 15<sup>th</sup> OWS and determine if a different method should be used. Current convective wind forecasting methods used by the 15<sup>th</sup> OWS include the T<sub>1</sub>, T<sub>2</sub>, and Snyder methods as stated in the Air Force Weather Agency's (AFWA) Tech Memo 98-002. Methods focused on in this thesis will be the T<sub>1</sub> and T<sub>2</sub> methods due to the high frequency of use by the 15<sup>th</sup>, and the Wind INDEX or WINDEX method which is a recently developed convective wind forecast method (McCann 1994). The T<sub>1</sub> and T<sub>2</sub> methods have been shown to provide an accurate wind forecast occasionally, but often times the methods are inaccurate depending on the convective situation. An in-depth analysis of the wind forecasting methods will hopefully aid in making current forecasts more accurate.

In addition to the primary goal of evaluating the current convective wind forecasting methods most often used by the 15<sup>th</sup> OWS, two secondary goals are listed below.

1. Compare the accuracy of the T1 and T2 methods and the WINDEX method for varying situations.
2. Examine the errors in model-derived convective wind forecasts to determine whether it is a problem with the methods themselves or the MM5 model output used to compute the T1, T2, and WINDEX wind gust values.

## **B. CONVECTIVELY DRIVEN HIGH WINDS**

When airmass conditions such as instability are sufficient to promote convective vertical motion in the atmosphere, air parcels become buoyant or less dense than surrounding air allowing the air parcels to rise. The air parcels cool rapidly as they rise until the parcel becomes saturated. Additional lifting of the air parcel results in condensation and leads to the formation of precipitation. Once precipitation formation has occurred, a fundamental element of a storm commonly forms: the convective downdraft (Wakimoto 2001).

The formation of the downdraft completes the atmosphere circuit of convective overturning by cooling and drying the boundary layer. When the downdraft reaches the surface it spreads out and sometimes produces a gust front at the leading edge. Occasionally, these downward motions and outflow of air can produce strong (35 knots – 49 knots) to severe (50 knots or greater) winds. These strong to severe winds can result in substantial crop, tree, and structural damage including military assets. The ability to detect and forecast these winds events is an ongoing challenge to operational forecasters (Wakimoto 2001).

### **1. Climatology of Damaging Wind Events**

A study presented by Kelly et al. (1985) examined 75,626 severe thunderstorms from 1955 through 1983. Of those events, 61% were wind-related events. These wind events have been found to be mainly a summertime phenomena. The months of June and July show the highest frequency of observed wind events (see Figure 1.2) while May and August also show a high occurrence of events. The wind events are divided into three categories based on measured wind speed. Violent gusts are defined as those above  $33.5 \text{ m s}^{-1}$ , strong gusts as between  $25.8$  and  $33.5 \text{ m s}^{-1}$ , and wind damage is the third group with no associated velocity (Kelly et al. 1985).

The diurnal variation of the three categories is shown in Figure 1.3 using normalized solar time (NST) to compensate for discontinuities in time zones.

Using NST allows one to compare events from different seasons and different locations. The peak time for thunderstorm wind events is late afternoon coinciding after the strongest daytime heating. A significant amount of activity is also seen between midnight and sunrise with a slight peak around midnight in all three categories (Kelly et al. 1985).

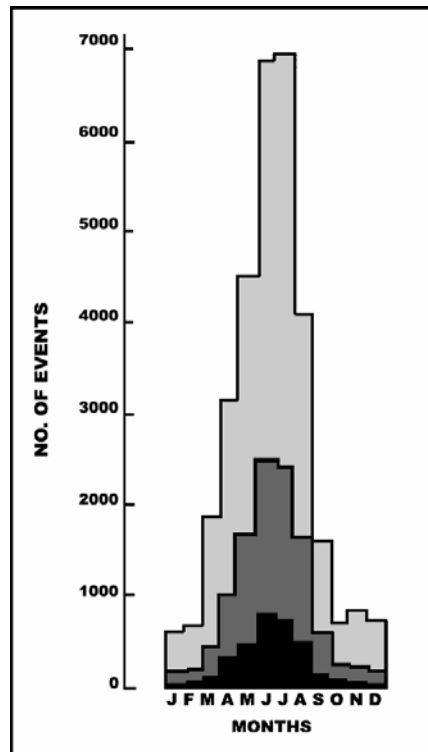


**Figure 1.2.** Monthly distribution of occurrences of thunderstorms related wind damaged (light gray) gusts between 25.8 and 33.5 m s<sup>-1</sup> (gray) and gusts greater than 33.5 m s<sup>-1</sup> (black) (After Kelly et al. 1985).

The spatial distribution of wind events across the United States is very complex with two major frequency axes (see Figure 1.4). One axis curves southeastward from southern Minnesota across Iowa, Illinois, Indiana, and Ohio. The other axis starts in central Texas and crosses Oklahoma and Kansas before turning eastward to the Kansas City region (Kelly et al. 1985). Due to a high probability of population bias, the values for the high plains and Arizona are likely underestimated.

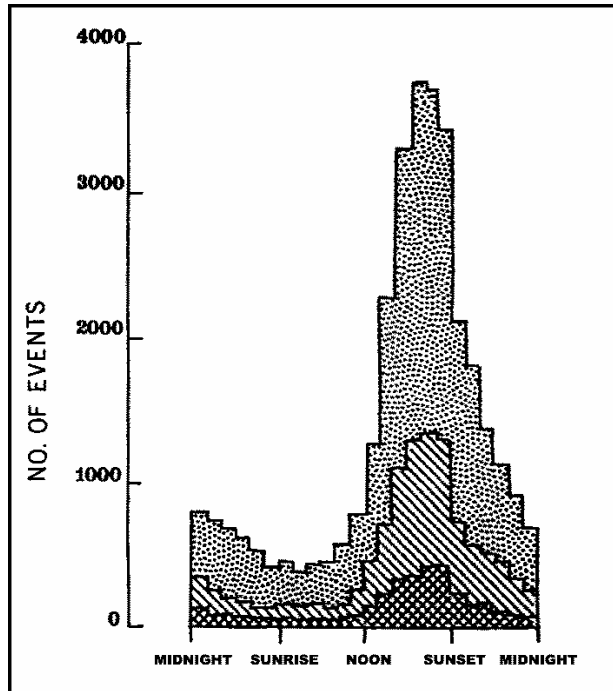


**Figure 1.3.** Hourly distribution in NST of occurrences of thunderstorm related wind damage (stippled) gusts between 25.8 and 33.5 m s<sup>-1</sup> (upper left to lower right hatching) and gusts greater than 33.5 m s<sup>-1</sup> (cross hatching) (From Kelly et al. 1985).

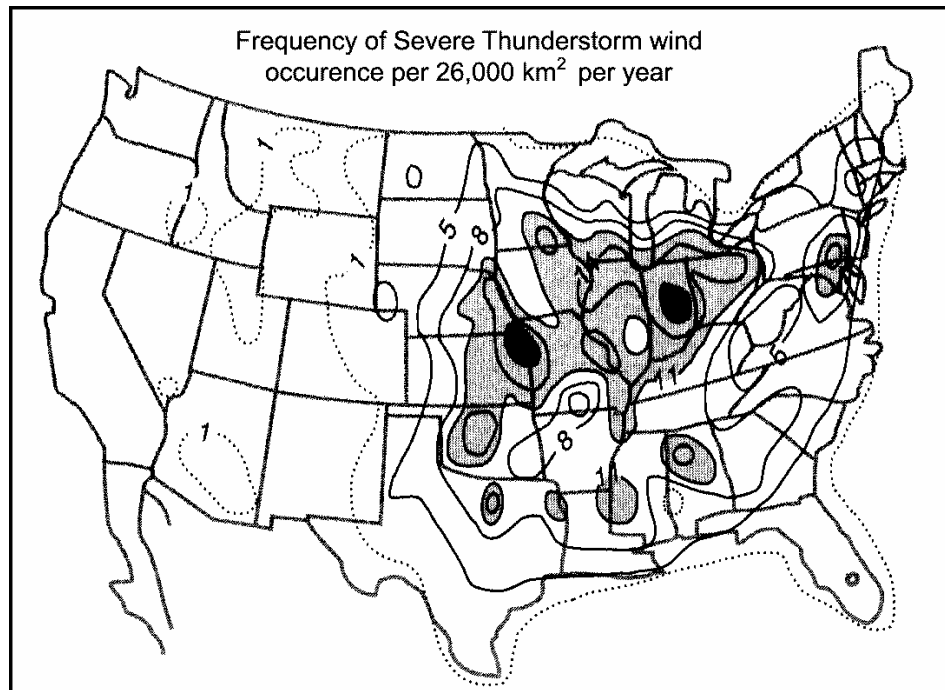


**Figure 1.4.** Dashed black lines are isopleths of one. Values greater than 11 and 17 are shaded gray and black, respectively (After Kelly et al. 1985).

## **2. Understanding the Downdraft**

It is important to understand what mechanisms go into creating a downdraft that causes damaging surface winds. The two fundamental areas of a thunderstorm are the updraft and downdraft. The updraft is super-saturated due to air constantly rising into it and cooling to its dewpoint temperature. Downdrafts are typically sub-saturated because of the condensate cooling by evaporation, melting, or sublimation all together does not make up for the amount of warming due to adiabatic cooling of the air. High wind events are often referred to as downbursts or microbursts (Wakimoto 2001).

Condensate loading, the process by which air is initially dragged downward by the weight of precipitation particles and then cooled by evaporation, can contribute to the initiation of the downdraft. The maintenance of a downdraft by falling precipitation is a function of drop size, rain intensity, and downdraft speed (Wakimoto 2001).

The microphysics within the downdraft is vital in determining the strength of the downdraft winds. For instance, small raindrops are more conducive to stronger downdrafts due to the increased surface area exposed to the environment versus a smaller number of larger drops. The smaller the drop diameter, the greater the curvature effect, resulting in a larger equilibrium vapor pressure which lowers relative humidity allowing for greater evaporative potential. However, it is possible for larger drops to produce a deeper, stronger downdraft if the rainwater mixing ratio is low enough and if the larger drops spread the cooling rapidly over a greater depth (Srivastava 1985)

Pressure buoyancy effects can also be significant in convective clouds. Pressure buoyancy means that an air parcel will accelerate upward if it is at a lower pressure than compared with the pressure of its surrounding environment. When compared to thermal buoyancy effects, the effects of pressure buoyancy are relatively weak. If the apparent updraft would happen to penetrate into the tropopause, the effect of pressure buoyancy would be more significant (Wakimoto 2001).



It has been shown that the incidence of intense downdrafts, driven only by evaporative cooling, are favored as the lapse rate of temperature gets closer to the dry-adiabatic lapse rate, if a high rainwater mixing ratio near cloud base exists, and the downdraft radius is at least 1 km. If the lapse rate of temperature becomes more stable, i.e. further away from the dry-adiabatic lapse rate, then intense downdrafts tend to only occur for only higher values of rainwater mixing ratio. Also, under stable environmental conditions, downbursts can be solely driven by the evaporation and melting of precipitation and by precipitation loading below cloud base (Srivastava 1987).

Lapse rate temperatures near the dry-adiabatic rate allow for intense downdraft formation even if little precipitation is present. Precipitation in the form of ice has been found to increase the intensity of downdrafts compared to precipitation in the form of rain. As the lapse rate becomes more stable, higher precipitation amounts, precipitation in the form of ice, and higher concentrations of smaller precipitation particles are needed to produce an intense downdraft (Srivastava 1987).

There are two different opinions on the effect that entrainment of air into the downdraft has on downdraft speeds. First, dry air entrainment is thought to actually promote downdrafts by evaporation or sublimation of cloudy air or precipitation. A second and less known theory is that entrainment of dry air actually reduces the downdraft speed by decreasing the virtual temperature difference. It has also been shown that stronger downdrafts develop when the environmental relative humidity is high. This goes against previous thoughts that high relative humidity should produce weaker downdrafts due to the decreased potential for evaporative cooling. If there were no entrainment, the relative humidity is then just determined by its initial condition instead of the environmental relative humidity. The virtual temperature differences between the air in the downdraft and the environment determine the vertical velocities within the downdraft. The difference is greater when the environmental relative humidity is high allowing for the increased downdraft speeds (Wakimoto 2001).

The size of downdrafts has an effect on the probable intensity of downdraft winds. Narrow downdrafts are typically weakened by turbulence, while larger downdrafts are weakened by pressure gradient forces contradicting buoyancy forces. A downdraft with a diameter of roughly 1 km is the optimal size to be the most efficient at producing strong downdraft winds. At this size, it is large enough to minimize impacts of entrainment, but small enough where pressure gradient forces are relatively unimportant (Proctor 1989).

The most essential part in driving a downburst is cooling due to the evaporation of rain. The next significant part is the cooling due to hail melting. When microphysical processes do not allow for cooling, a downburst can be driven primarily by mass loading due to the weight of the precipitation. If no cooling existed, downdrafts driven by mass loading are typically much weaker than if cooling did exist (Proctor 1988).

Essentially, studies have concluded that most downdrafts are driven by cooling from phase changes as rain evaporates and hail melts. Condensate loading and entrainment can be thought as a trigger in initiating downward motion, however; entrainment has been shown to reduce downward velocities in lower levels.

### **3. Types of Downdrafts**

The gust front is the essential component to the production of strong to severe winds at the surface. A gust front occurs when a downdraft reaches the surface, spreads out and undercuts warmer air at the surface. The leading edge of the outflow of cooler air undercutting the warmer surface air is called a gust front (see Figure 1.5). The figure shows the motion of air depicted by arrows. The cold air is shown to approach the gust front from within the outflow, but is deflected vertically in a counter-clockwise motion. Air ahead of the gust front is typically warmer and is forced over the approaching cold air often forming what is known as a shelf, roll, rope, or arc cloud (Wakimoto 2001).

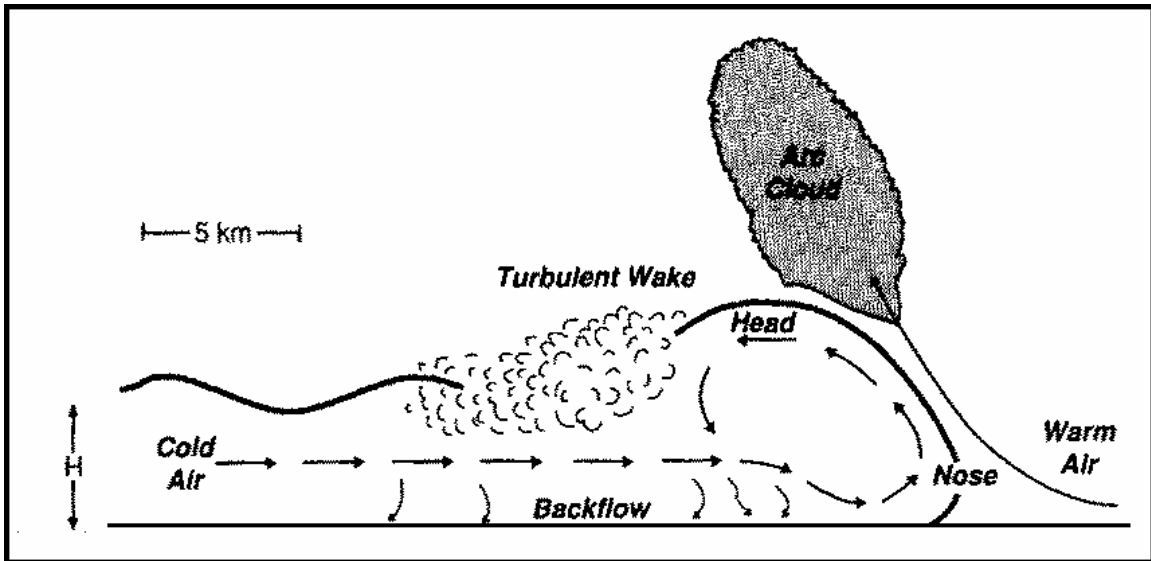


**Figure 1.5.** Schematic cross section through the gust front of a thunderstorm (After Wakimoto 2001).

A supercell thunderstorm is typically the most violent type of thunderstorm. Two types of downdrafts originate from a supercell: the forward-flank downdraft and the rear-flank downdraft (see Figure 1.6). The forward-flank downdraft occurs downwind of the updraft core and within the precipitation area. The outflows associated with these downdrafts are not typically strong, but is an important contributor to the formation of the low-level mesocyclone. The rear-flank downdraft is the strongest of the two associated with a supercell. It has been found to be formed as the low-level mesocyclone intensifies, lowering the pressure locally. The lowered pressure near the surface allows for air to be drawn down from above producing the rear-flank downdraft (Wakimoto 2001).

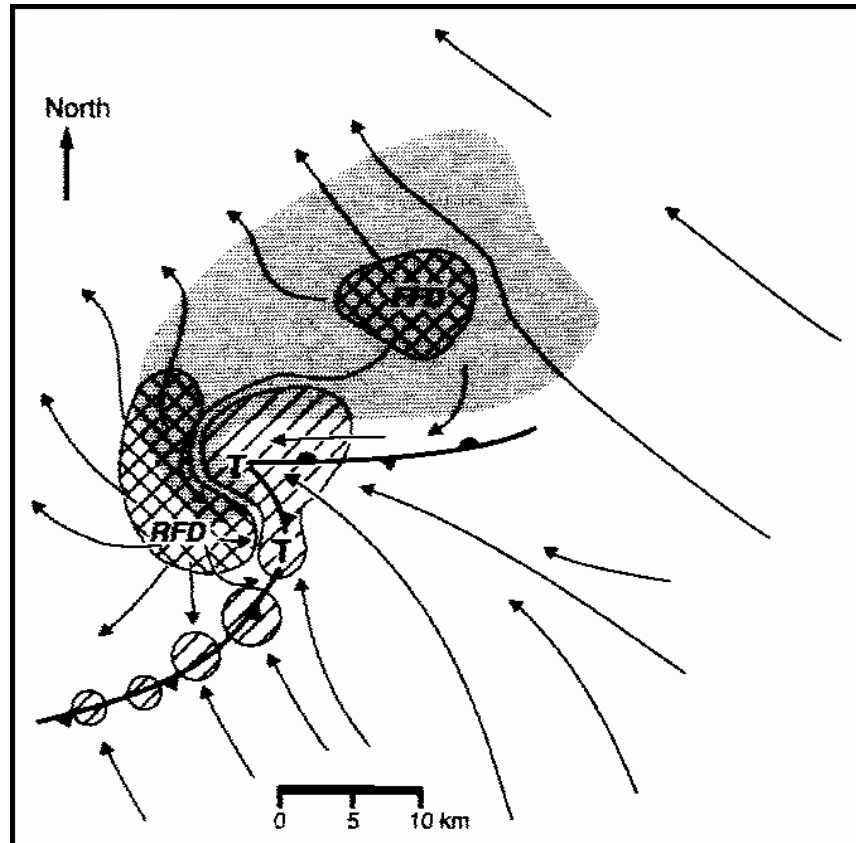


**Figure 1.6.** Schematic view of the supercell thunderstorm at the surface. The gray shading encompasses the radar echo. The gust front structure is depicted using a solid line and frontal symbols. Surface position of the updraft is hatched while the forward-flank downdraft (FFD) and rear-flank downdraft (RFD) are crosshatched (From Wakimoto 2001).

Thunderstorms sometimes produce microburst downdrafts with documented wind speeds up to 180 knots. Microbursts are very common, but most are not severe. A mid-air microburst may descend and hit the surface spreading out in all directions. The outer edges of the microburst outflow often produce rotor areas as the outflow spreads out (see Figure 1.7). Severe microbursts have been known to cause extensive crop, tree, and structural damage, and also have been the cause for several aircraft accidents (Wakimoto 2001).

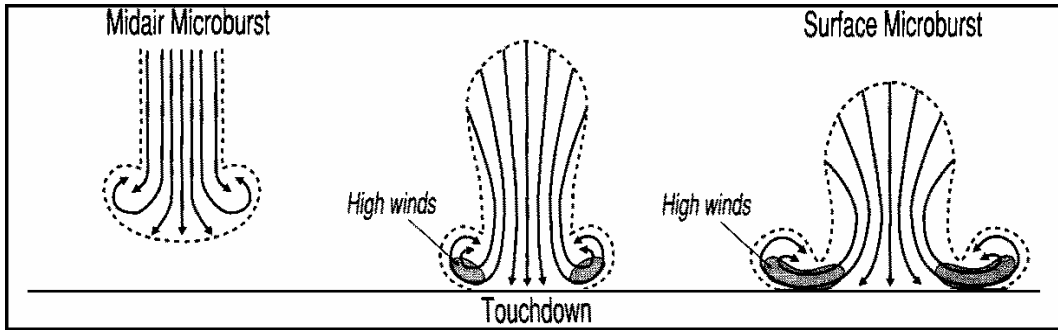


**Figure 1.7.** Conceptual model of a microburst hypothesized to explain ground damage patterns. Three stages of development are shown. A midair microburst may or may not descend to the surface. If it does, the outburst winds develop immediately after reaching the surface (From Wakimoto 2001).

Mesoscale downdrafts are associated with mesoscale convective systems (MCS). An MCS is a convective system on a horizontal scale of 100 km or more. Included within MCS are groups of convective storms and squall lines. Squall lines can form strong cells within that produce intense convective downdrafts driven by precipitation loading and evaporative cooling. Another type of mesoscale downdraft producing event resulting in a family of downbursts is referred to as a derecho. Derechos are described as long-lived convective systems in the form of long bow-shaped segments of cells. Bow-echoes within a derecho can cause widespread severe winds causing damage for hundreds of miles during the lifetime of a derecho. The shape of a bow-echo is caused by a strong rear-inflow jet with its core at the apex of the bow causing the cell to accelerate and bulge out where the rear-inflow jet impacts it (see Figure 1.8) (Wakimoto 2001).

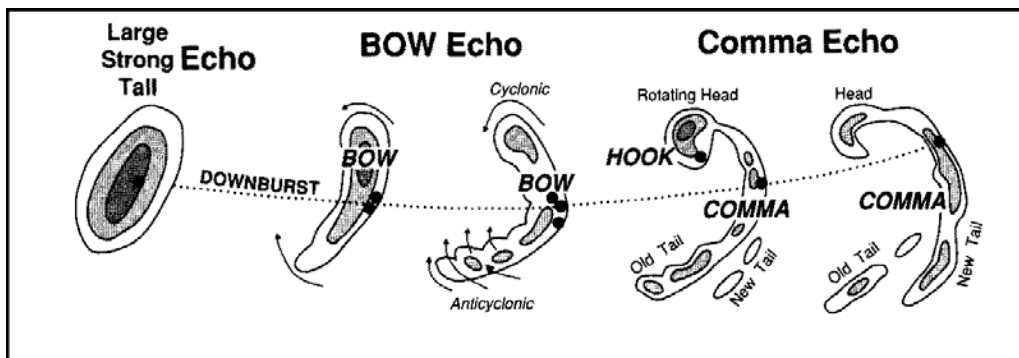


**Figure 1.8.** A typical evolution of radar echoes associated with bow echoes that produce strong and extensive downbursts (From Wakimoto 2001).

THIS PAGE INTENTIONALLY LEFT BLANK

## II. TECHNIQUE

### A. OVERVIEW OF CONVECTIVE WIND FORECASTING METHODS

Concerns over being able to forecast the occurrence of damaging wind events led to the development of two convective wind forecasting methods by Ernest J. Fawbush and Robert C. Miller over 50 years ago (Fawbush and Miller 1954). The original method developed is now known as the  $T_2$  method while the  $T_1$  method was developed later. Recently, a new convective wind forecasting method has been developed by Donald W. McCann called WINDEX which is more representative of the downdraft dynamics for the three methods (McCann 1994).

#### 1. $T_1$ Gust Method

Fawbush and Miller developed the  $T_1$  method, also referred to as the Dry Instability Index, with the intent of giving forecasters a way to estimate maximum thunderstorm wind gusts. This method is mainly used when thunderstorm coverage is isolated or scattered. The data used to compute  $T_1$  is taken from a current or forecasted upper air sounding close to the forecast area. The procedure to find the  $T_1$  value is found in the Air Weather Service's Technical Report 200 and is as follows:

a. If the sounding has an inversion, the moist adiabat is followed from the warmest point in the inversion to 600 millibars. The difference between the temperature of the moist adiabat at the 600 mb level and the observed temperature of the dry bulb at 600 mb on the sounding is  $T_1$ . The inversion point should be within 150 or 200 mb of the surface and must not be susceptible to becoming wiped out by surface convection.

b. If no inversion appears on the sounding, or if the inversion is relatively high (more than 200 mb above the surface), a different method is used to find  $T_1$ . The maximum temperature at the surface is forecast in the usual manner. A moist adiabat is projected from the maximum temperature to the

600 mb level. The difference between the temperature of the moist adiabat at the 600 mb level and the dry-bulb temperature observed at 600 mb is  $T_1$ .

To find a forecasted maximum wind gust from the computed  $T_1$  value, Table 2.1 is used. The wind gust value from Table 2.1 also needs to be added to one-third of the mean wind speed expected in the lower 5000 feet above the ground. This final wind speed is then the expected maximum wind gust from scattered thunderstorms in the vicinity of the forecast location.

**Table 2.1.**  $T_1$  convective gust potential (After Miller 1972).

<b><math>T_1</math> values (°C)</b>	<b>Average Gust Speed (knots)</b>	<b><math>T_1</math> values (°C)</b>	<b>Average Gust Speed (knots)</b>
3	17	15	49
4	20	16	51
5	23	17	53
6	26	18	55
7	29	19	57
8	32	20	58
9	35	21	60
10	37	22	61
11	39	23	63
12	41	24	64
13	45	25	65
14	47		

## **2. $T_2$ Gust Method**

Fawbush and Miller developed the  $T_2$  method in the early 1950s. Data used to develop the method were taken from 62 different non-frontal



thunderstorm events passing over reporting stations. It was found that there was a correlation between the surface temperature, the ambient temperature just preceding the storm and the temperature immediately following the first heavy shower, the downrush temperature (Fawbush and Miller, 1954). The  $T_2$  method is most useful when it is applied to squall lines or numerous thunderstorms.

From the Air Weather Service's Technical Report 200, the  $T_2$  value is found by first locating the  $0^\circ\text{C}$  isotherm on the wet-bulb curve of an upper air sounding. A moist adiabat through that point is followed down to the surface and the temperature at that point is recorded. This temperature is subtracted from the dry-bulb temperature, or the free-air temperature giving the value of  $T_2$ . To find the gust potential from the computed  $T_2$  value, figure 2.1 is used. The left most curve on the figure is the maximum wind gust expected, while the middle curve is the average gust and the right most curve is the minimum gust expected.

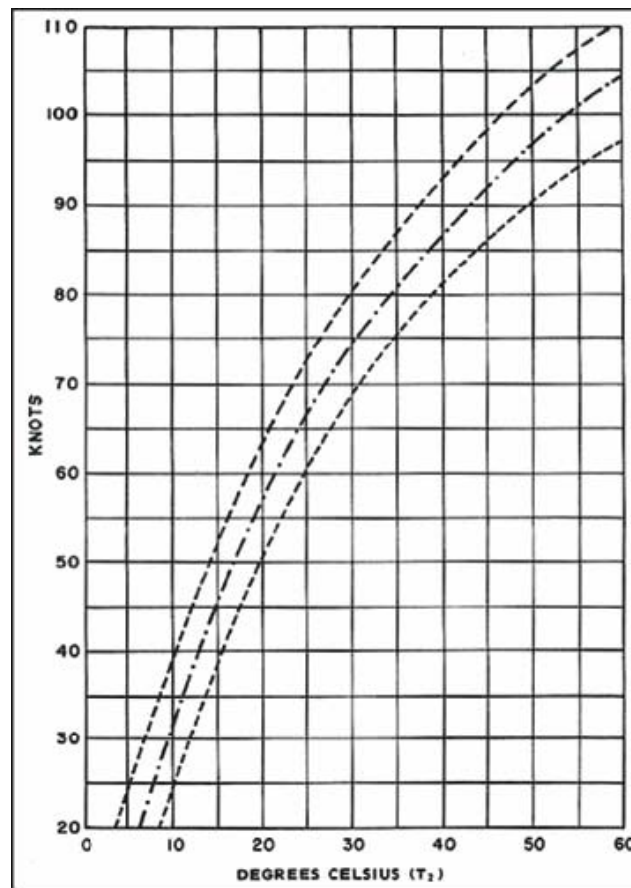


**Figure 2.1.** Given a calculated  $T_2$  value, wind gust potential can be estimated using the curves (After Miller 1972)

### 3. WINDEX Gust Method

The WINDEX method was introduced to identify air masses favorable for microbursts and is a measure of downdraft instability (McCann 1994). The method can be computed using atmospheric soundings from current environmental conditions or from numerical weather prediction models. Microburst development mainly originates between the melting level and the surface as frozen precipitation falls through the melting level causing air parcels to cool. Air parcels then become negatively buoyant and accelerate downward with evaporation continuing as parcels fall to the surface. As a result, the lapse rate between the melting level and the surface is an important part of how WINDEX is computed. WINDEX is represented by WI and is computed in knots using the following parameters;  $H_M$  is the height of the melting level in km above the surface;  $\Gamma$  is the lapse rate in degrees Celsius per kilometer from the surface to the melting level;  $Q_L$  is the average mixing ratio in the lowest 1 km above the surface;  $Q_M$  is the mixing ratio at the melting level; and  $R_Q = Q_L / 12$  but not greater than 1:

$$WI = 5[H_M R_Q (\Gamma^2 - 30 + Q_L - 2Q_M)]^{0.5} \quad (2.1)$$

The lapse rate within the WINDEX equation is very important, especially for values smaller than  $5.5^\circ\text{C km}^{-1}$  because the computed WINDEX value will be set as zero. In an environment where the lapse rate is less than  $5.5^\circ\text{C km}^{-1}$ , microburst probabilities are basically zero. The WINDEX equation is most sensitive to the environmental lapse rate due to the theory that the steeper the sounding lapse rate, the stronger the downdraft because air parcels will be more negatively buoyant. For WINDEX to be the most accurate, secondary convection such as convection involving outflow boundaries from primary conditions would be involved. WINDEX values will likely be overestimated due to the fact that microbursts are typically weaker associated with primary convection (McCann 1994).

### III. DATA AND METHODS

#### A. DATA USED

##### 1. Storm Reports

To evaluate the various forecast indices, strong to severe wind gust reports were obtained from two different sources for the months of June and July of 2005, from the Storm Prediction Center's (SPC) database and actual reports from observation stations (<http://www.spc.noaa.gov/climo/>). Reports from north latitude of 38 degrees and west longitude of 104 degrees were used to encompass the 15<sup>th</sup> OWS AOR. The SPC database is an archive of daily storm reports which includes thunderstorm wind reports of 50 knots or greater. Some reports include a numerical recorded wind gust value which can be estimated by a trained spotter or from a wind observational device. The majority of the wind reports are reported as UNK (unknown wind gust speed). These reports were also recorded but do not provide substantial value since a true gust value is not known. The reports are listed each day based from 12Z on the current day until 12Z the following day. A sample SPC storm report map is shown in Figure 3.1 where severe wind gusts are shown as blue dots or black squares.

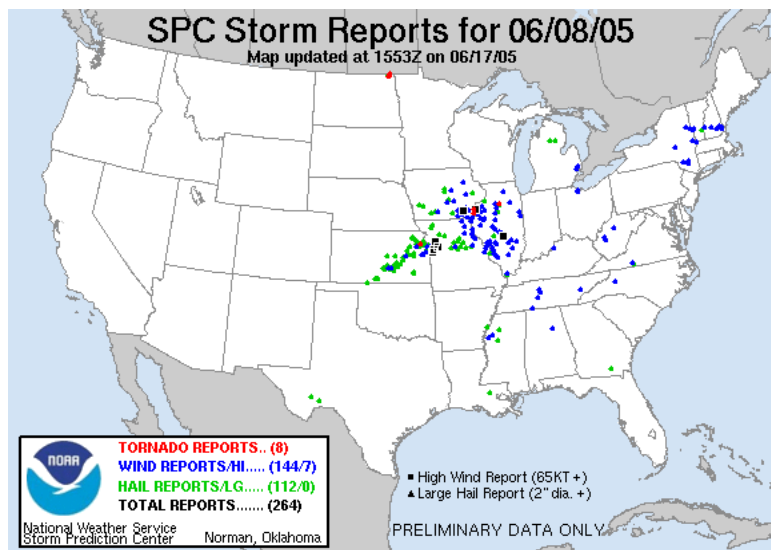


**Figure 3.1.** Sample SPC storm report map from 08 June 2005 (From Ref. Storm Prediction Center Severe Weather Events Archive, <http://www.spc.noaa.gov/climo/>, February 2006)

Storm reports from SPC were used to provide accurate location in latitude and longitude coordinates and time of the report to match up with model data. An example list of reports from 08 June 2005 is shown in Table 3.1 with the speed in miles per hour and an unknown wind speed displayed as UNK. Archived data reports were also compiled from recorded wind gusts from observation stations across the selected region of study.

**Table 3.1.** Example of storms reports from SPC from 08 June 2005 (After Ref. Storm Prediction Center Severe Weather Events Archive, <http://www.spc.noaa.gov/climo/>, February 2006)

Time	Speed	Location	County	State	Lat	Lon	Comments
1955	58	2 W Delavan	Tazewell	IL	4037	8958	Measured wind gust 58 mph (ILX)
2000	UNK	Peoria	Peoria	IL	4074	8961	9 inch live tree limb fell on van (ILX)
2044	62	11 NE St. Charles	St. Charles	MO	3890	9037	Recorded by set ASOS (LSX)
0023	64	Macomb Township	Macomb	MI	4267	8292	21 mile/card Rd (DTX)
0028	60	10 SSE Council Grove	Morris	KS	3853	9642	(TOP)
0040	62	Richmond	Macomb	MI	4281	8275	Wind gust damaged roof to car dealership (DTX)
0107	65	1 E Ottawa	Franklin	KS	3862	9525	(TOP)

Once the storm reports from the SPC database and additional reports of 35 knots or greater from observation stations were compiled, the cause of the gusts had to be verified as resulting from a thunderstorm. Using archived NEXRAD reflectivity imagery (see Figure 3.2) from the National Climatic Data Center (NCDC), the compiled storm wind gusts were referenced with the reflectivity data to verify thunderstorms were in the vicinity of the reported gust (<http://www4.ncdc.noaa.gov/cgi-win/wwcgi.dll?WWNEXRAD~Images2>).

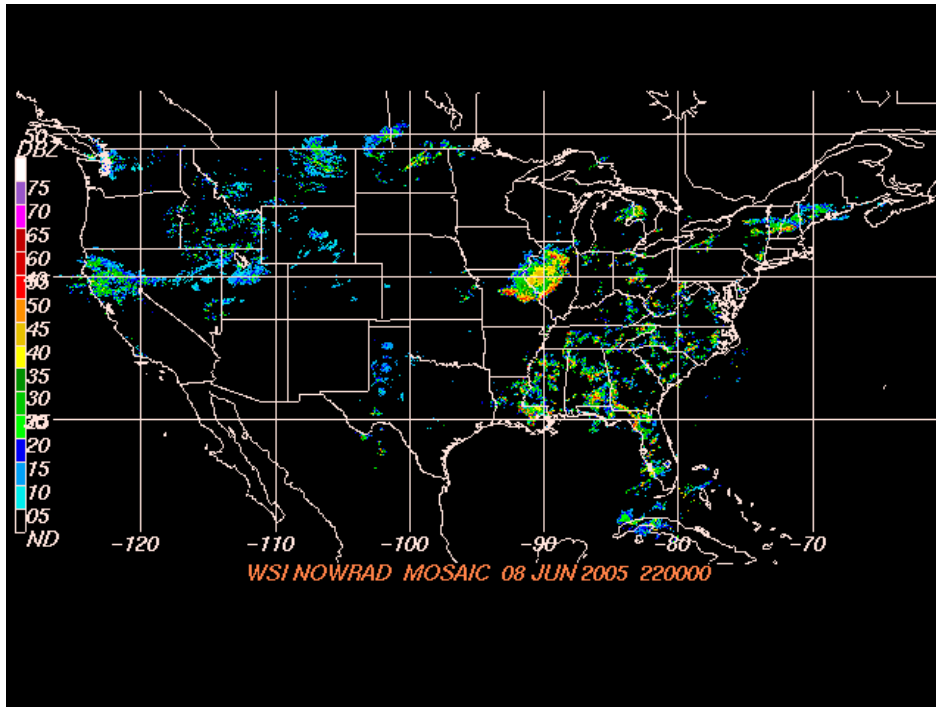


**Figure 3.2.** Sample of NEXRAD imagery from 08 June 2005 at 22Z (From Ref. National Climatic Data Center, <http://www4.ncdc.noaa.gov/cgi-win/wwcgi.dll?WWNEXRAD~Images2>, February 2006)

## 2. Model Data

After the SPC storm reports and the observation reports from June and July were assembled with latitude and longitude coordinates labeled on each report, model data was then used to calculate the wind gust forecast. The selected model data is from the AFWA MM5 model with 15 km grid resolution. The MM5 is a non-hydrostatic grid-point model that consists of a 15 km horizontal resolution and 42 sigma levels of vertical resolution, however, only 23 pressure levels in the vertical are used to disseminate the forecast for operational use (<http://meted.ucar.edu/nwp/pcu2/index.htm>). The model uses a six hour data assimilation window starting at 06Z and 18Z to produce six hour forecasts that are essentially an initial analysis at 12Z and 00Z with output at three hourly intervals after that time. Storm reports 90 minutes before and after a MM5 forecast time used data from that particular forecast time for comparison. For instance, a storm report that occurred at 2215Z is closer to the forecast output time of 21Z than 00Z, so the model data from the 15 hour forecast from the 06Z

run would be used. The 06Z model runs were used for reports between 1330Z and 0129Z and the 18Z model runs were used for reports between 0130Z and 1329Z.

## **B. DATA PROCESSING**

### **1. Method Calculations**

The known location of reported convective wind gusts in latitude and longitude coordinates and the exact time of occurrence are important to be able to compute wind gust estimates using the MM5 model data for each wind gust method. The procedures for each method to calculate wind gusts use upper air data from the model at each horizontal grid point. The resolution of the AFWA MM5 model is 15 km which means each observed wind gust location had to be assigned to the closest horizontal grid point in the model. Assigning each observed wind gust location to the nearest model grid point is not expected to degrade the accuracy of the wind gust computation method since the gusts are calculated no more than 11 km from the actual location of the report.

To calculate  $T_1$  gusts from the MM5 model, the vertical profile in the model at each horizontal grid point at each output time was used. Based on the  $T_1$  calculating procedures noted earlier and referencing procedures in the AFWA Technical Manual 98-002, a possible temperature inversion had to be accounted for. This was done by finding the maximum temperature in the lowest 200 mb by checking the first eight vertical grid points. If the surface temperature is the highest, then that is used. The  $T_1$  procedure states that the forecast maximum temperature is to be used; however, the application to the model data only uses the warmest current temperature at the forecast hour near the time of the report. This may slightly skew computed values for events that did not occur close to the daily maximum surface temperature, but using the highest temperature in the lowest 200 mb accounts for the lower surface temperatures during the overnight and early morning hours. The warmest temperature in the lowest 200 mb is then lifted to 600 mb along the corresponding moist adiabat. The  $T_1$  value is obtained by finding the difference between the actual 600 mb temperature and the temperature after the warmest level is lifted moist adiabatically. Utilizing

Table 2.1, an initial wind gust value is determined from the  $T_1$  value. The background mean flow is accounted for by adding one-third of the average wind speed in the lowest eight model levels which is close to the lowest 5000 feet stated in the procedure. Adding the initial wind gust value and the calculated background mean flow, gives an estimated  $T_1$  wind gust very close to location of the observed wind gust report.

To calculate  $T_2$  gusts from the MM5 model fields, the first step is to determine the wet-bulb zero level. Using the wet-bulb temperature profile, the level closest to zero degrees Celsius is found in the vertical at each horizontal grid point. The moist adiabat that passes through the temperature and pressure of the level closest to the wet-bulb zero is then used to find the corresponding moist adiabatic temperature in degrees Celsius at the surface. This temperature is then subtracted from the model surface temperature to get a  $T_2$  value in degrees Celsius. Using Figure 2.1, the minimum, average, and maximum expected wind gusts can be estimated using the curves. This procedure was done for the closest horizontal grid point to each observed wind gust report providing an estimated  $T_2$  wind gust.

The calculation of WINDEX for all wind reports is based on Equation 2.1. To calculate WINDEX, the mixing ratio at the freezing level, the average mixing ratio in the boundary layer and the average surface to freezing level lapse rate temperature must be determined. The model grid level closest to zero degree Celsius is determined by searching vertically through the model profile. Once found, the height and mixing ratio of the grid point is determined. The boundary layer mixing ratio is found by averaging the first six model levels together. The model surface temperature or the warmest temperature in the lowest six vertical levels is used to calculate the average lapse rate to the freezing level. These values are then used in Equation 2.1 to calculate a WINDEX estimated wind gust at each horizontal grid point in the model.

## **2. Upper Air Soundings**

The  $T_1$  and  $T_2$  convective wind forecasting methods utilized observed upper air soundings when the methods were first developed. For example, an

observed upper air sounding taken at 12Z would be used along with a forecasted maximum temperature to determine the gust potential for any thunderstorms that would form during the afternoon. The benefit of using observed soundings is that the true atmospheric conditions are known for a location. However, there are also problems with using observed soundings. Typically, observed upper soundings are only taken twice daily, at 12Z and 00Z, so it is hard to get the true atmospheric conditions due to time restrictions. Another pitfall to observed soundings is there are few locations where the soundings are taken throughout the country. Essentially, you could have a thunderstorm in a location where the closest observed sounding station is over a hundred miles away, thus calling into question the similarities of the two environments.

Current convective wind forecasting methods often make use of model-derived soundings. Model soundings can be generated for any horizontal grid point location which is often much closer to a thunderstorm's location than an actual observed sounding location. Another benefit of model soundings is the ability to actually get a forecast of the atmospheric conditions many hours before a thunderstorm develops. For example, the AFWA MM5 has the ability to provide forecast soundings at any grid location every three hours. This allows forecasters to get an idea of the atmospheric conditions and to actually compute potential thunderstorm wind gusts before a thunderstorm develops. However, there is one major fault with model-derived soundings; it is solely based on a forecast model. Forecast models are all far from perfect in predicting the exact atmospheric conditions for a particular location and time. If the model is not accurate in producing an upper air sounding, the model forecasted gust values for the  $T_1$ , and  $T_2$ , and WINDEX methods will also not be accurate.

To illustrate the potential errors in determining model derived gust parameters, let's examine an observed and model sounding. Figure 3.3 is a 00Z observed sounding produced from launching a weather balloon with a radiosonde taking measurements of the atmospheric conditions. Figure 3.4 is a model-derived forecast sounding from the MM5 06Z model run also valid at 00Z for the same location as the observed sounding. The cyan line represents the



temperature and the magenta line represents the dewpoint. The temperature profile between the two soundings is quite different with a strong inversion shown near the surface on the observed sounding and no inversion on the model sounding. The inversion is not extremely important for  $T_1$  and WINDEX since the maximum temperature in the lowest 200 mb is used, but this poses a big problem for computing  $T_2$  since it is dependent on the surface temperature. Looking at the temperature profile overall, the observed sounding's temperature is much colder between 850 mb and 600 mb than the model sounding. This means the model sounding is underestimating the potential instability in the mid-levels of the atmosphere. The dewpoint structure of both soundings also varies significantly with the observed sounding much drier in the lower levels and more moist in the mid-levels. Due to the uncertainty in the model's ability to predict an accurate vertical profile of the atmosphere, it is difficult to consistently predict thunderstorm wind gusts with accuracy.

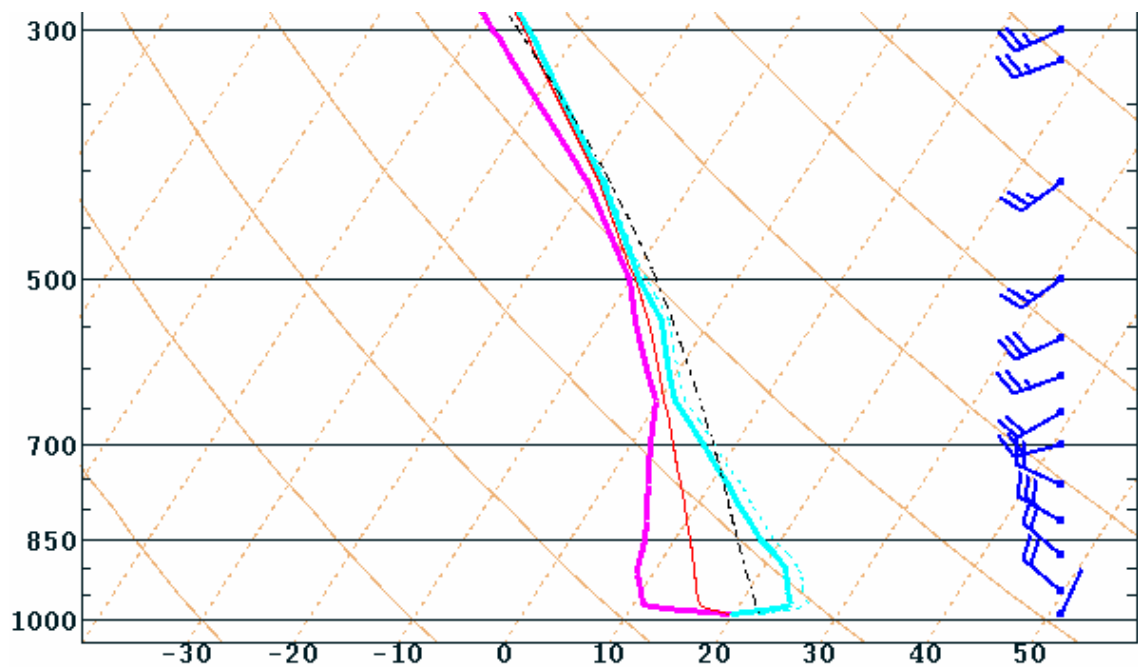


**Figure 3.3.** Observed atmospheric sounding from 00Z. Pressure in millibars on the left and temperature in degrees Celsius on the bottom

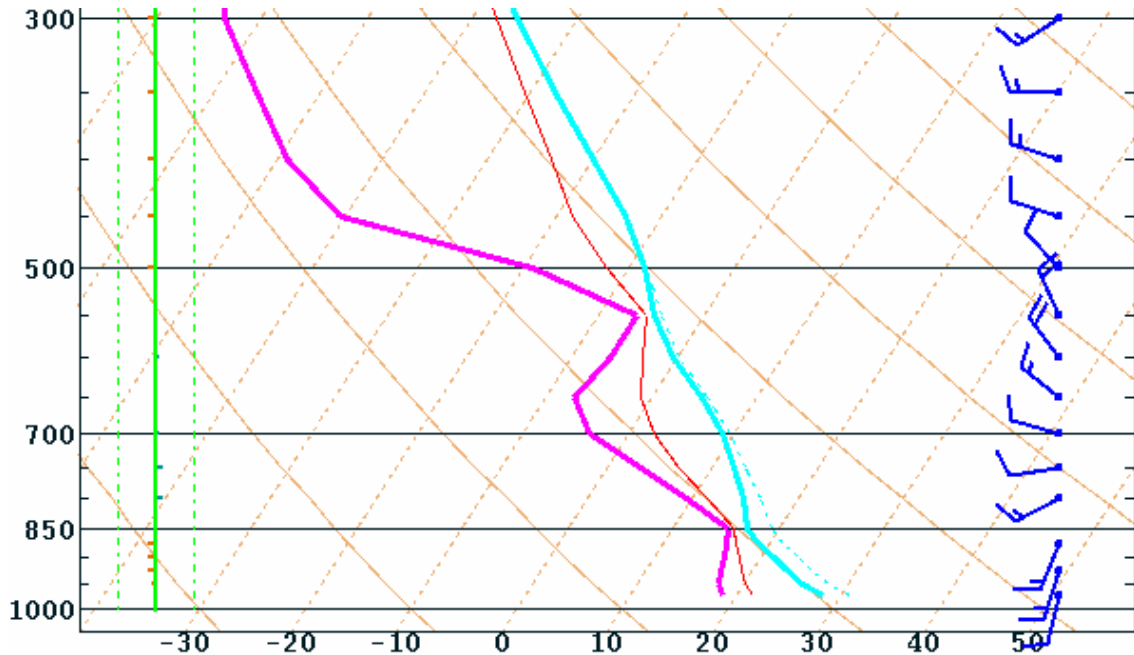


**Figure 3.4.** MM5 06Z model run sounding valid at 00Z. Pressure in millibars on the left and temperature in degrees Celsius on the bottom

### 3. Visual Program

The VISUAL program is a FORTRAN program developed by Prof. Wendell Nuss to display meteorological data. The program is based on NCAR Graphics and XGKS graphical software for plotting data. The program enables a variety of computations to be performed on a gridded dataset with also the ability to plotting the grids. Plotting the computed  $T_1$ , and  $T_2$ , and WINDEX wind gusts in contour intervals of every 10 knots across the 15 OWS AOR was accomplished for each three hour forecast interval. Figure 3.5 shows WINDEX computed wind gusts in 10 knot contour intervals. Dark areas represent wind gusts of less than 10 knots, light blue areas represent gusts between 10 and 30 knots, while green areas represent gusts greater than 30 knots. The actual observed gust reports are overlaid on the image in knots while unknown wind speeds are represented by the letter 'U'. It is interesting to see packing in the contour lines especially through western Minnesota, western Iowa, and eastern Nebraska providing evidence of frontal boundaries.

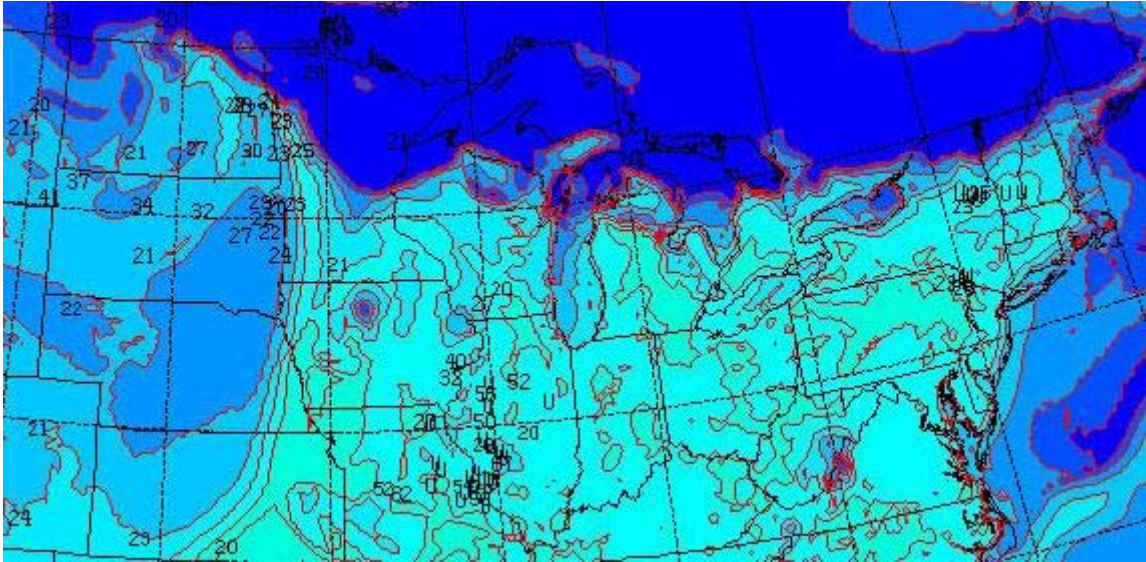


**Figure 3.5.** Example of computed WINDEX gusts with dark blue colors representing low wind gusts and dark green colors representing high wind gusts. Contour intervals every 10 knots

THIS PAGE INTENTIONALLY LEFT BLANK

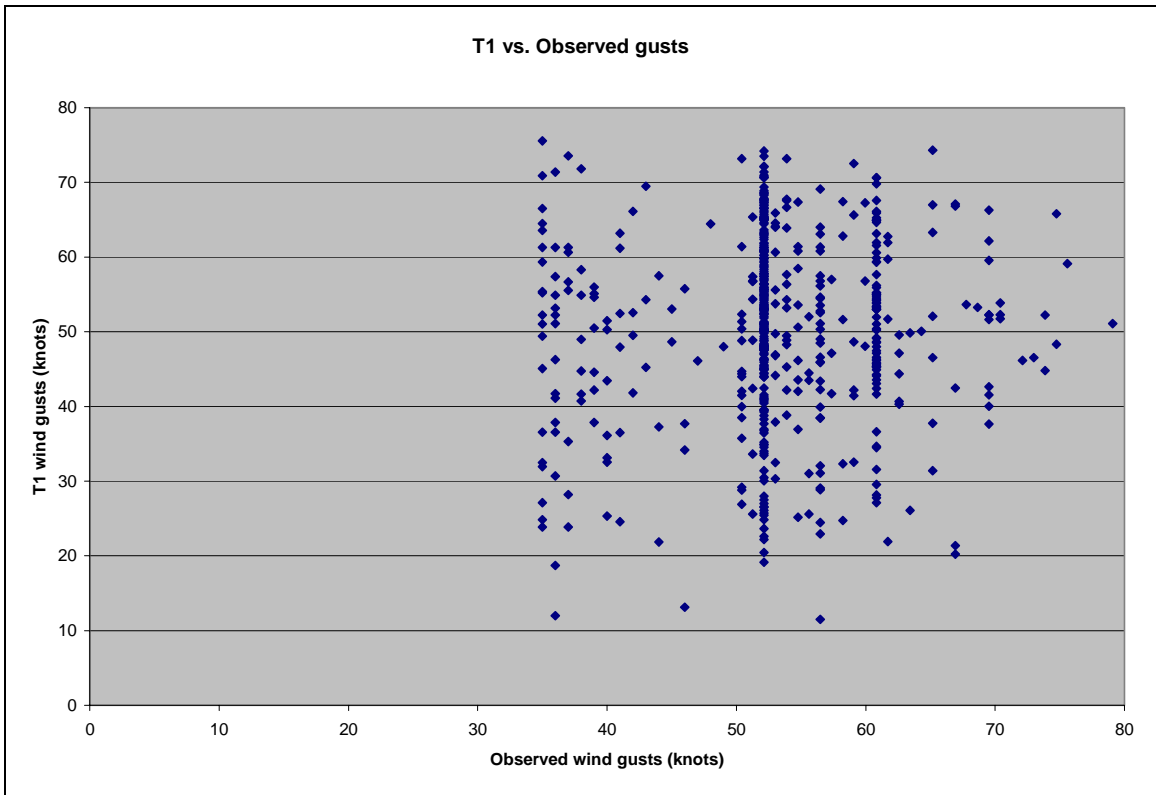
## IV. DATA ANALYSIS

### A. OVERALL RESULTS

A total of 941 storm reports above 35 knots from June and July of 2005 were catalogued for this study. The storm reports were separated into a  $T_1$  section and a  $T_2$  section. This was done by checking the storm type using NEXRAD radar. Isolated and scattered thunderstorm coverage in the area of the wind report was labeled as  $T_1$ , while wind reports in the vicinity of squall lines, bow echoes, and numerous thunderstorms were labeled as  $T_2$ . The WINDEX method was computed for each wind report. The majority of the storm reports came from late afternoon to early evening thunderstorms across the eastern Great Plains, the Midwest, and Ohio River Valley. This thunderstorm coverage is not unexpected based on thunderstorm climatology for the area studied shown in Figure 1.3 and Figure 1.4.

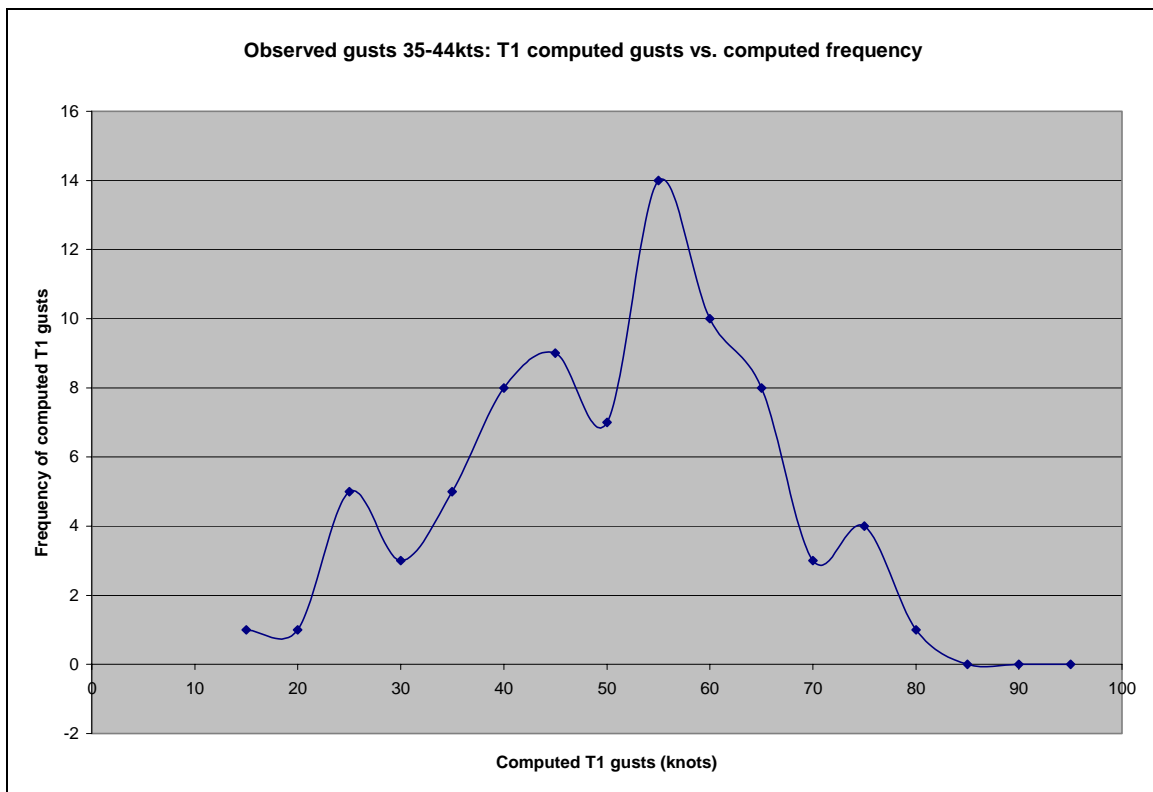
#### 1. $T_1$ Gust Method

There were 554 storm reports classified under the  $T_1$  gust method. A computed  $T_1$  value for each storm report was found by processing the MM5 model data. A plot of all reports for June and July is shown in Figure 4.1., which compares each observed storm report with its computed  $T_1$  gust value in knots. The spread for the  $T_1$  gusts is from 10 knots to 80 knots, but the majority of the values calculated are between 40 and 60 knots. The figure shows visible vertical banding where observed gusts tend to group, corresponding with 60, 65, and 70 mph wind speeds. The abnormal amount of observed wind reports at the three gust values calls into question the validity of the speeds of the gusts themselves. This suggests that many of the observed wind gust reports are likely to be estimated wind speeds showing that the dataset be not be entirely accurate itself. A scatter line sloped to the upper right of the plot would prove the  $T_1$  method to be accurate; however, the slope of the scatter plots is shown to be relatively flat. A flat slope to the scatter plot shows the lack of correlation between the computed  $T_1$  gusts to the observed gusts.



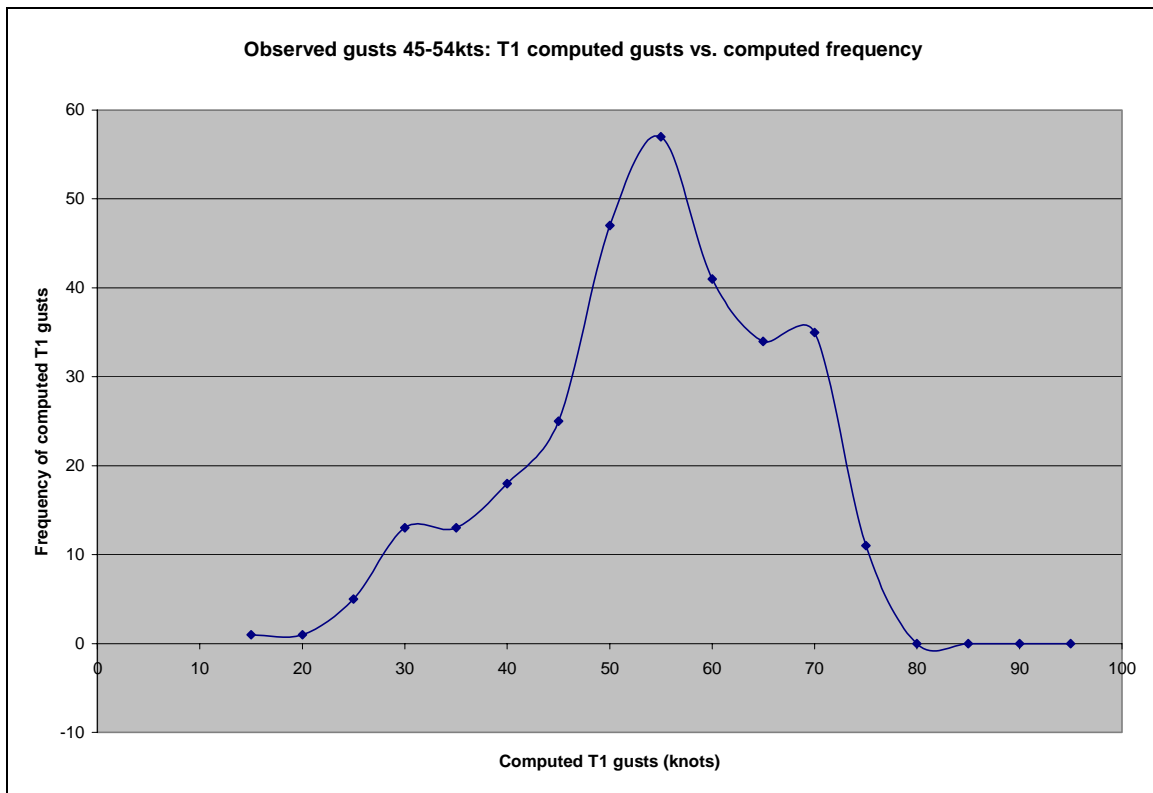
**Figure 4.1.** Computed T1 gust value versus observed wind gusts for June and July of 2005.

To investigate the spread in  $T_1$  forecasts for a given range of observed gusts, frequency charts were constructed. Figure 4.2 shows the frequency of computed  $T_1$  gust values for the observed storm reports between 35 and 44 knots. For each storm report between 35 and 44 knots the computed  $T_1$  gust value was divided into a set of ranges: less than 15 knots, 15 to 20 knots, 21 to 25 knots, and so on up to 90 knots in 5 knot increments. The frequency of computed  $T_1$  gusts was compiled for each 5 knot increment and plotted. Figure 4.2 shows the highest frequency of computed  $T_1$  gust values fell between 51 to 55 knots with a second peak between 41 to 45 knots. A reliable forecast would be a Gaussian curve with spread no larger than the observed range. The figure does show a reasonable distribution, but the spread of the computed gusts is too high. The mean gust value is also too high showing that for observed gusts in this range, the  $T_1$  gust method tends to overestimate the wind gusts.



**Figure 4.2.** For observed reports between 35-44 knots: Computed  $T_1$  wind gusts are compared to the frequency of times computed it was computed within the range of observed gusts.

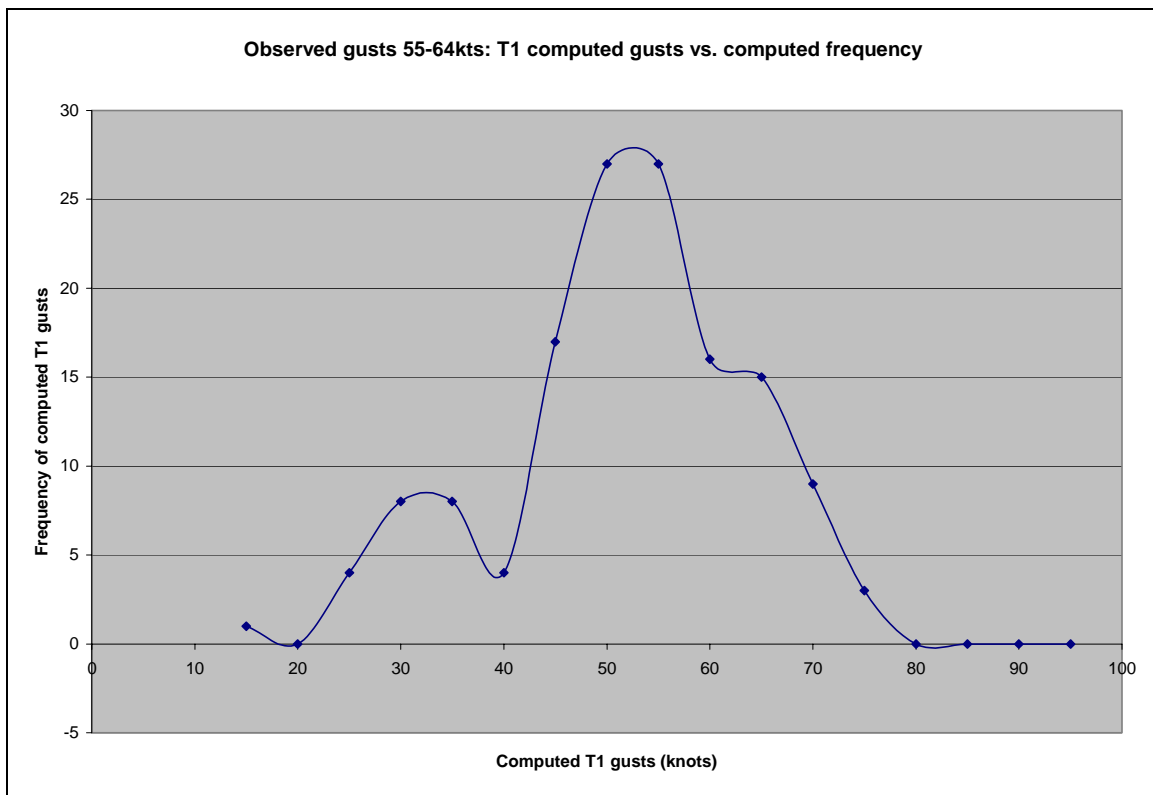
Figure 4.3 shows the frequency of computed  $T_1$  gust values for the observed storm reports between 45 and 54 knots. Figure 4.3 shows the highest frequency of computed  $T_1$  gust values fell between 51 to 55 knots. The peak occurrence for this range of observed wind gusts was overestimated, but showed improvement over the 35 to 44 knot range. The distribution of computed gusts is tighter than the previous discussed observed gust range suggesting greater accuracy in this gust range.



**Figure 4.3.** For observed reports between 45-54 knots: Computed  $T_1$  wind gusts are compared to the frequency of times computed it was computed within the range of observed gusts.

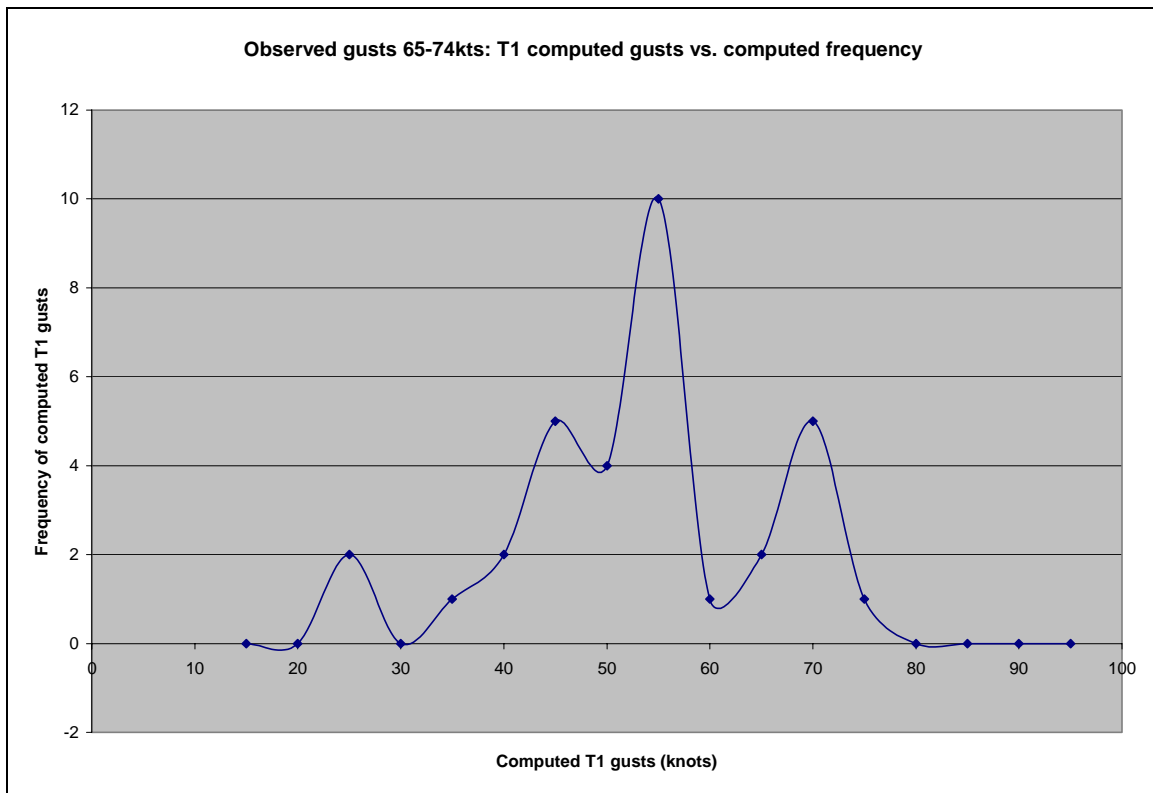


Figure 4.4 shows the frequency of computed  $T_1$  gust values for the observed storm reports between 55 and 64 knots. The figure shows the highest frequency of computed  $T_1$  gust values fell between 46 to 55 knots. The peak occurrence for this range of observed wind gusts was underestimated which is a turn around from previous ranges. The underestimate is likely due to the tendency for  $T_1$  to not predict extreme gusts. This is evident by the low number of predicted gusts above 65 knots. The individual horizontal plots also tend not to produce many areas above 60 to 70 knots.



**Figure 4.4.** For observed reports between 55-64 knots: Computed  $T_1$  wind gusts are compared to the frequency of times it was computed within the range of observed gusts.

Figure 4.5 shows the frequency of computed  $T_1$  gust values for the observed storm reports between 65 and 74 knots. The figure shows the highest frequency of computed  $T_1$  gust values fell between 51 to 55 knots with two secondary peaks between 41 and 45 knots and 66 and 70 knots. The peak occurrence for this range of observed wind gusts was underestimated once again, but the secondary peak of 66 to 70 knots is encouraging that the method is trying to produce forecasts in the correct range.

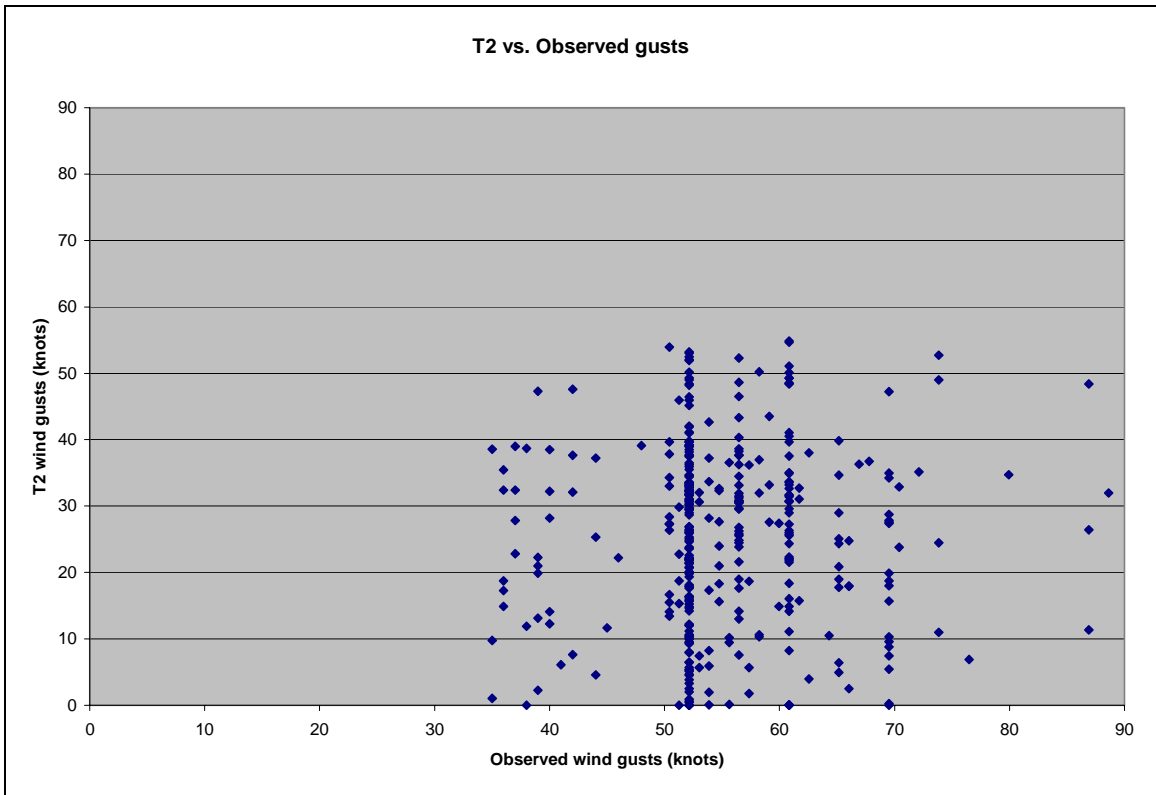


**Figure 4.5.** For observed reports between 65-74 knots: Computed  $T_1$  wind gusts are compared to the frequency of times it was computed within the range of observed gusts.

The frequency of computed  $T_1$  gust values for the observed storm reports between 75 and 90 knots was also computed. The computed  $T_1$  values were between 51 and 60 knots, which are more underestimated than other observed gust ranges; however, this may be due to the fact that there are only 2 storm reports for this range and so any statistical inference would not be reliable or even feasible.

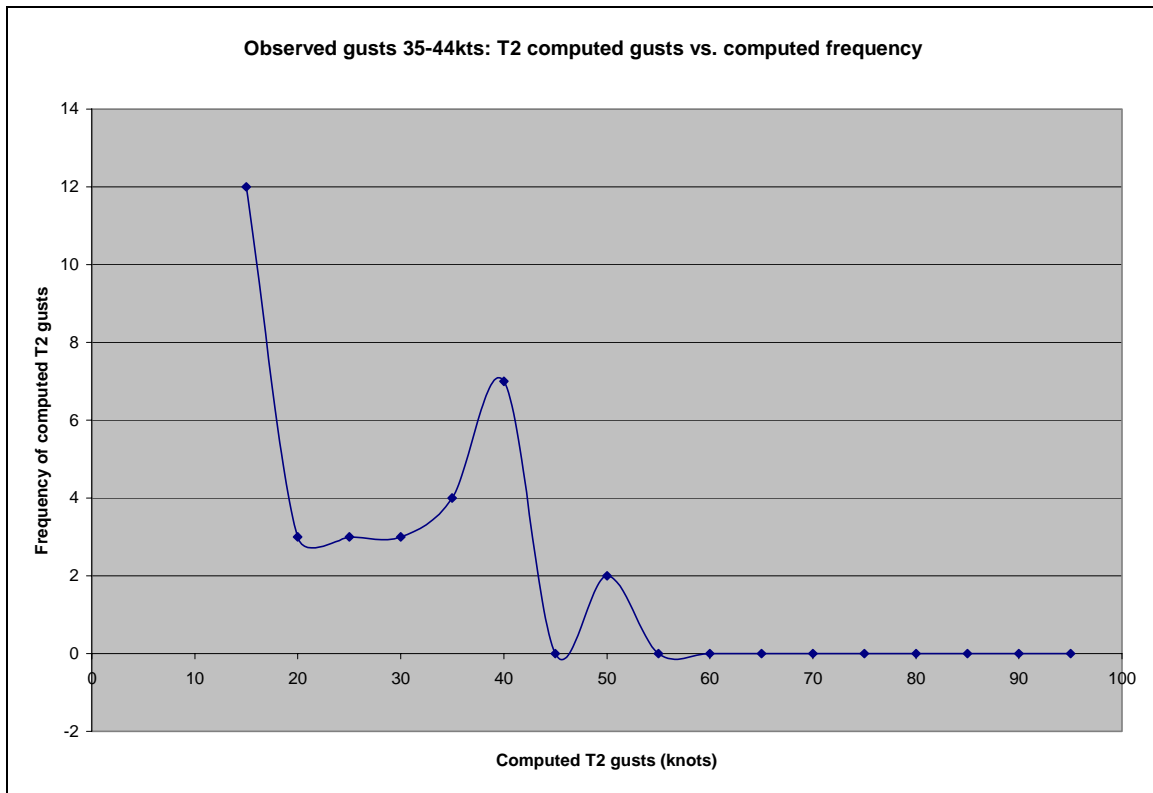
## **2. $T_2$ Gust Method**

There were 387 storm reports classified under the  $T_2$  gust method. A computed  $T_2$  value for each storm report was found by processing the MM5 model data. A plot of all reports for June and July are shown in Figure 4.6, which compares each observed storm report with its computed  $T_2$  gust value in knots. The spread for the  $T_2$  gusts is from 0 to 60 knots, but the majority of the values calculated are between 20 and 40 knots. The computed values are very low compared to most of the observed gust reports. The low values are likely due to calculations using the method during the evening or overnight hours. Surface temperatures during this time are normally unrepresentative of the actual boundary layer temperatures due to cooling at the surface. Consequently, the  $T_2$  method as applied to model forecasts shows a nighttime bias and will result in low wind estimates due to the cooler surface temperatures.



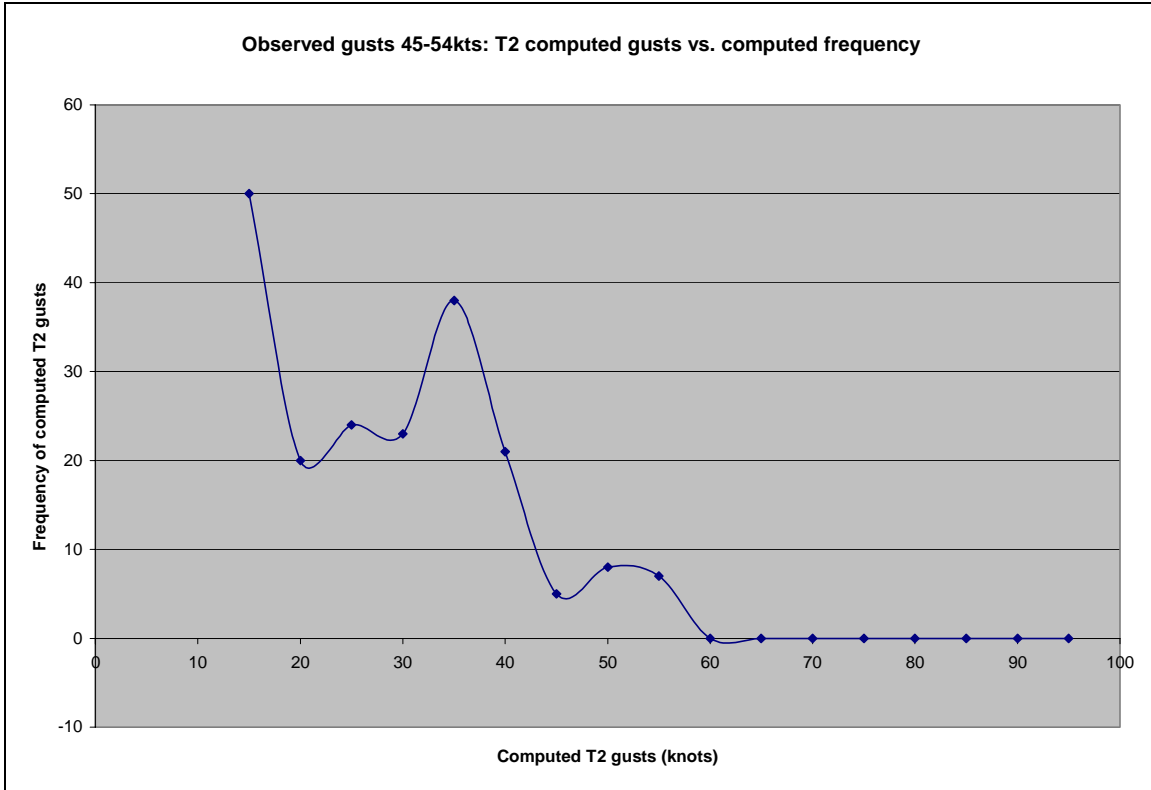
**Figure 4.6.** Computed T2 gust value versus observed wind gusts for June and July of 2005.

As with  $T_1$ , frequency charts were constructed to assess the ability of the forecast method to capture the observed variability. Figure 4.7 shows the frequency of computed  $T_2$  gust values for the observed storm reports between 35 and 44 knots. For each storm report between 35 and 44 knots the computed  $T_2$  gust value was divided into a set of ranges: less than 15 knots, 15 to 20 knots, 21 to 25 knots, and so on up to 90 knots in 5 knot increments. The frequency of computed  $T_2$  gusts was compiled for each 5 knot increment and plotted. Figure 4.8 shows the highest frequency of computed  $T_2$  gust values fell between 0 to 15 knots with a second peak between 36 to 40 knots. The highest frequency of less than 15 knots is most likely due to the nighttime bias of colder surface temperatures. The secondary peak of 36 to 40 knots is encouraging, especially if it is primarily representative of the daytime reports.



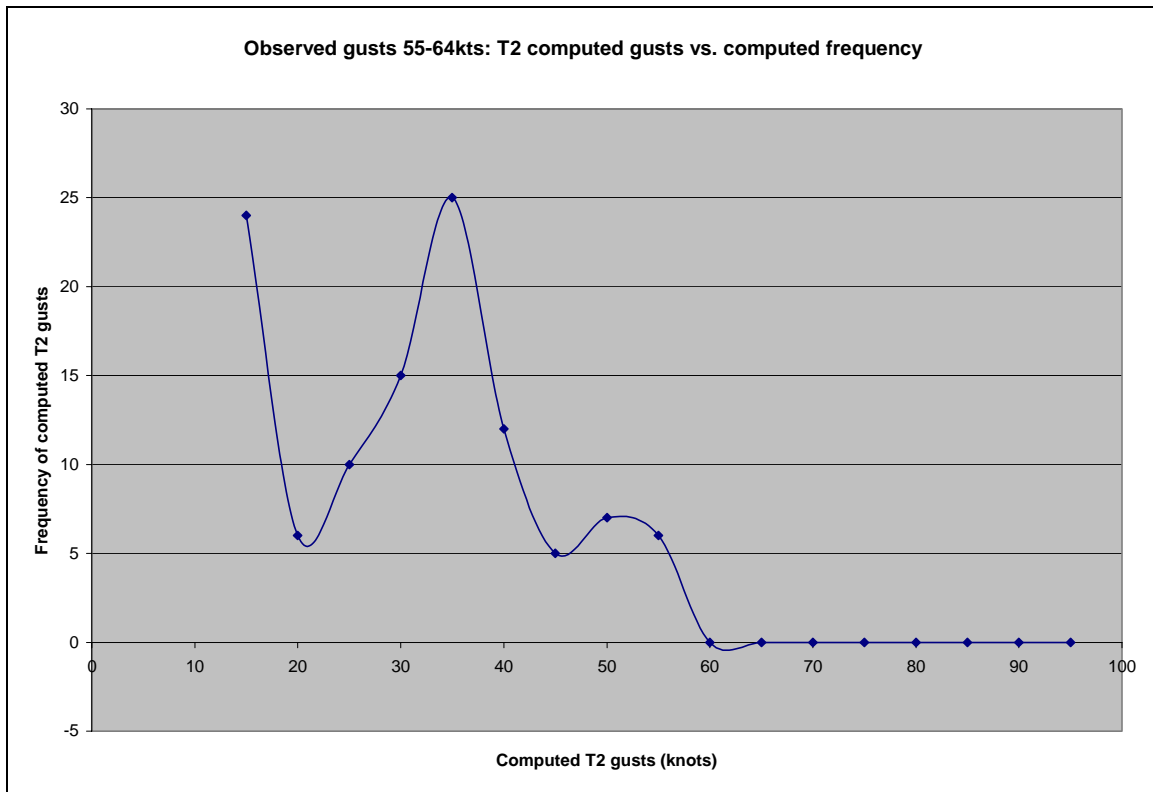
**Figure 4.7.** For observed reports between 35-44 knots: Computed  $T_2$  wind gusts are compared to the frequency of times it was computed within the range of observed gusts.

Figure 4.8 shows the frequency of computed  $T_2$  gust values for the observed storm reports between 45 and 54 knots. The highest frequency of computed  $T_2$  gust values once again fell between 0 and 15 knots, but this is likely due to the nighttime temperature bias. However, a secondary peak of 36 to 40 knots shows the  $T_2$  method is underestimating wind gusts, even during the more favorable daytime forecast hours.



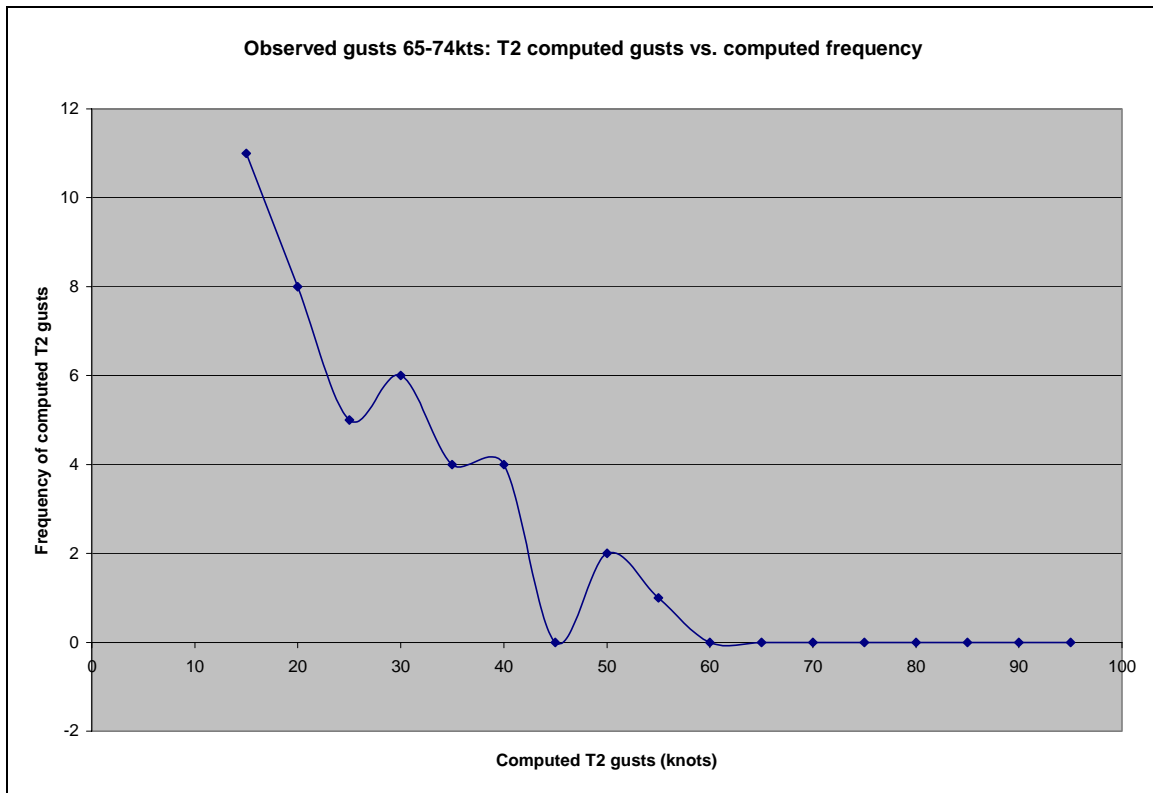
**Figure 4.8.** For observed reports between 45-54 knots: Computed  $T_2$  wind gusts are compared to the frequency of times it was computed within the range of observed gusts.

Figure 4.9 shows the frequency of computed  $T_2$  gust values for the observed storm reports between 55 and 64 knots. The high frequency of values below 15 knots is still there due to the nighttime bias, but the highest frequency of computed  $T_2$  gust values fell between 36 and 40 knots. This peak is still drastically below the observed gust range by an average of 20 knots, which suggests that the model-derived  $T_2$  forecasts have some consistent bias.



**Figure 4.9.** For observed reports between 55-64 knots: Computed  $T_2$  wind gusts are compared to the frequency of times it was computed within the range of observed gusts.

Figure 4.10 shows the frequency of computed  $T_2$  gust values for the observed storm reports between 65 and 74 knots. The high frequency of values below 15 knots is still there due to the nighttime bias, but there is no other distinct peak to provide useful information. The number of observed reports for this range is not enough to draw many conclusions. Even with the small number of reports, it is obvious that the method is still underestimating the wind gusts as there are no forecasts above 60 knots. There were only 6 reports to compute  $T_2$  gust values for the observed storm reports between 75 and 90 knots. Due to the small sample size there is not sufficient data to draw conclusions. All of the computed  $T_2$  gust values for observed gusts between 75 and 90 knots were still underestimated.

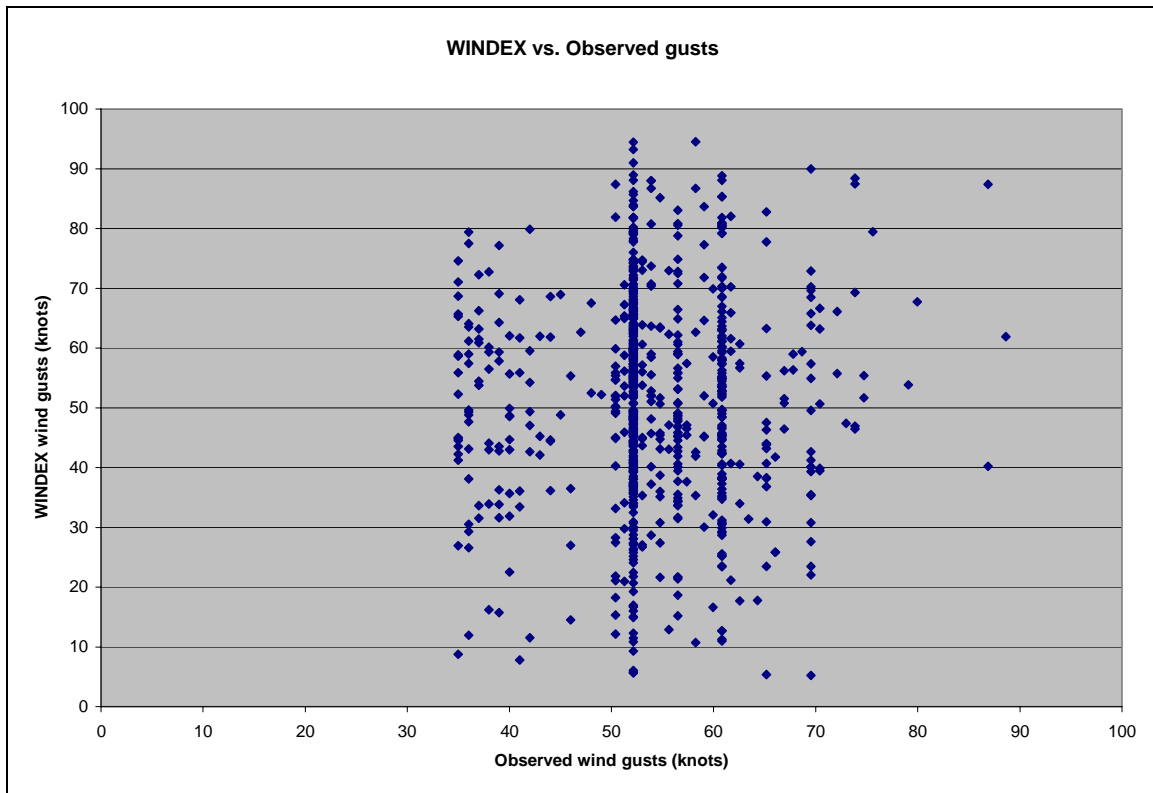


**Figure 4.10.** For observed reports between 65-74 knots: Computed  $T_2$  wind gusts are compared to the frequency of times it was computed within the range of observed gusts.



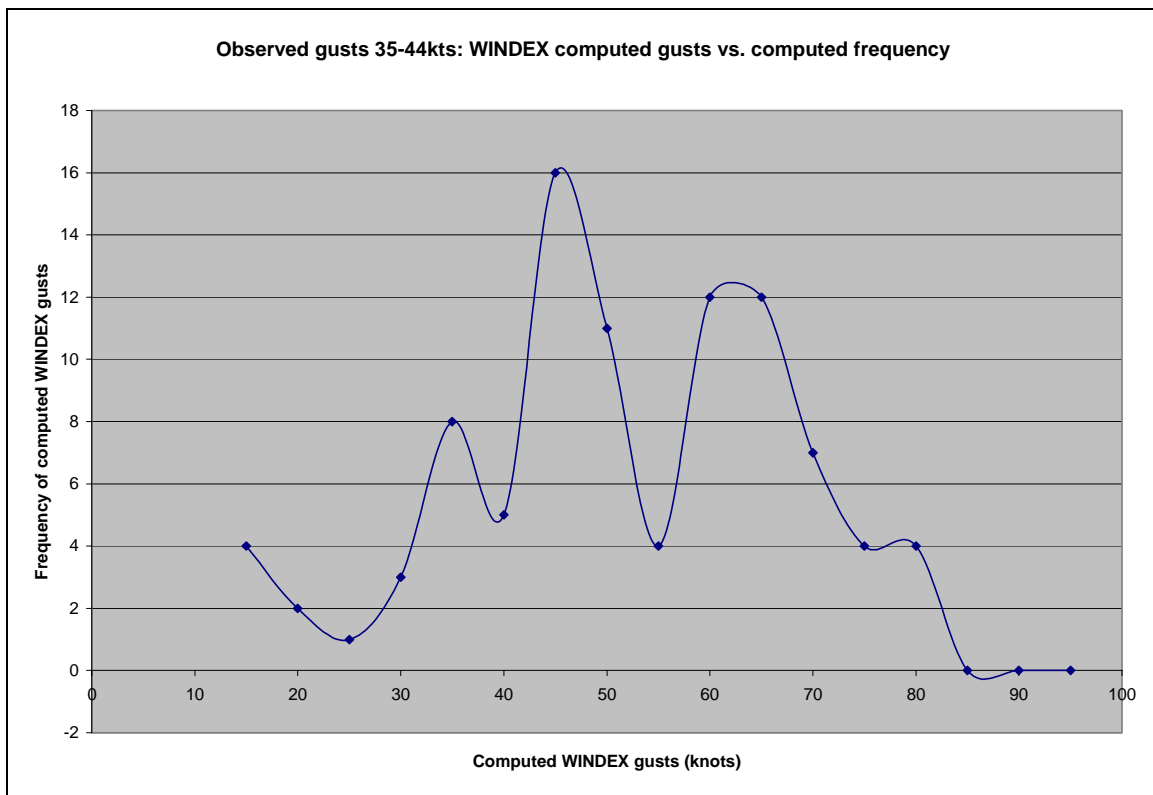
### 3. WINDEX Gust Method

The WINDEX method was run for the entire set of 941 storm reports. A computed WINDEX value for each storm report was found by processing the MM5 model data. A plot of all reports for June and July are shown in Figure 4.11, which compares each observed storm report with its computed WINDEX gust value in knots. Computed values of less than five knots were omitted due to the equation used to calculate WINDEX creates values near zero when the environmental lapse rate is less than  $5.5^{\circ}\text{C km}^{-1}$ . The spread for the computed gusts is from 5 to 95 knots, but the majority of the values calculated are between 30 and 70 knots. The lack of an obvious trend in the plot suggests that WINDEX forecasts are poorly correlated with observed wind gusts.



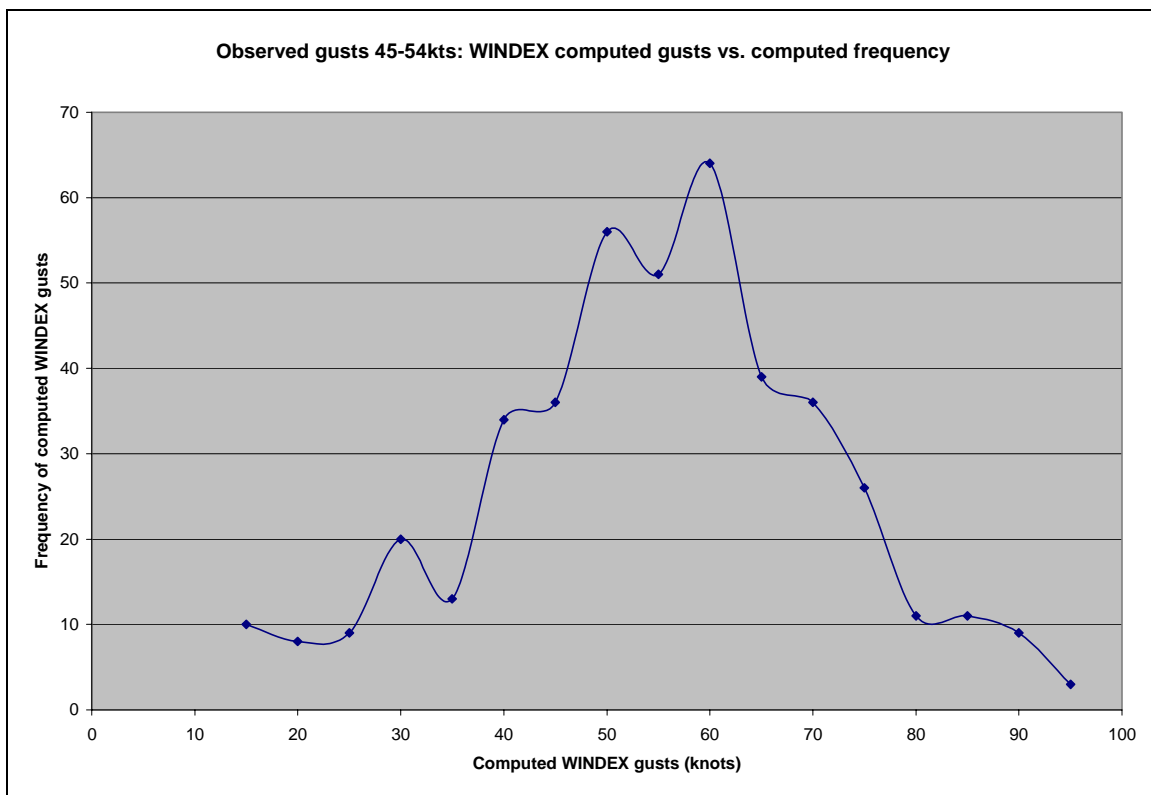
**Figure 4.11.** Computed WINDEX gust value versus observed wind gusts for June and July of 2005.

To access the statistical character of WINDEX forecasts, similar frequency charts to  $T_1$  and  $T_2$  were constructed. Figure 4.12 shows the frequency of computed WINDEX gust values for the observed storm reports between 35 and 44 knots. The figure shows the highest frequency of computed gust values fell between 41 to 45 knots with a second peak between 56 to 65 knots. The highest frequency falls in the range showing that the WINDEX method might provide a reliable estimate most frequently. However, the broad spread and second peak indicates the method is skewed to higher values and will tend to overestimate the gust forecasts.



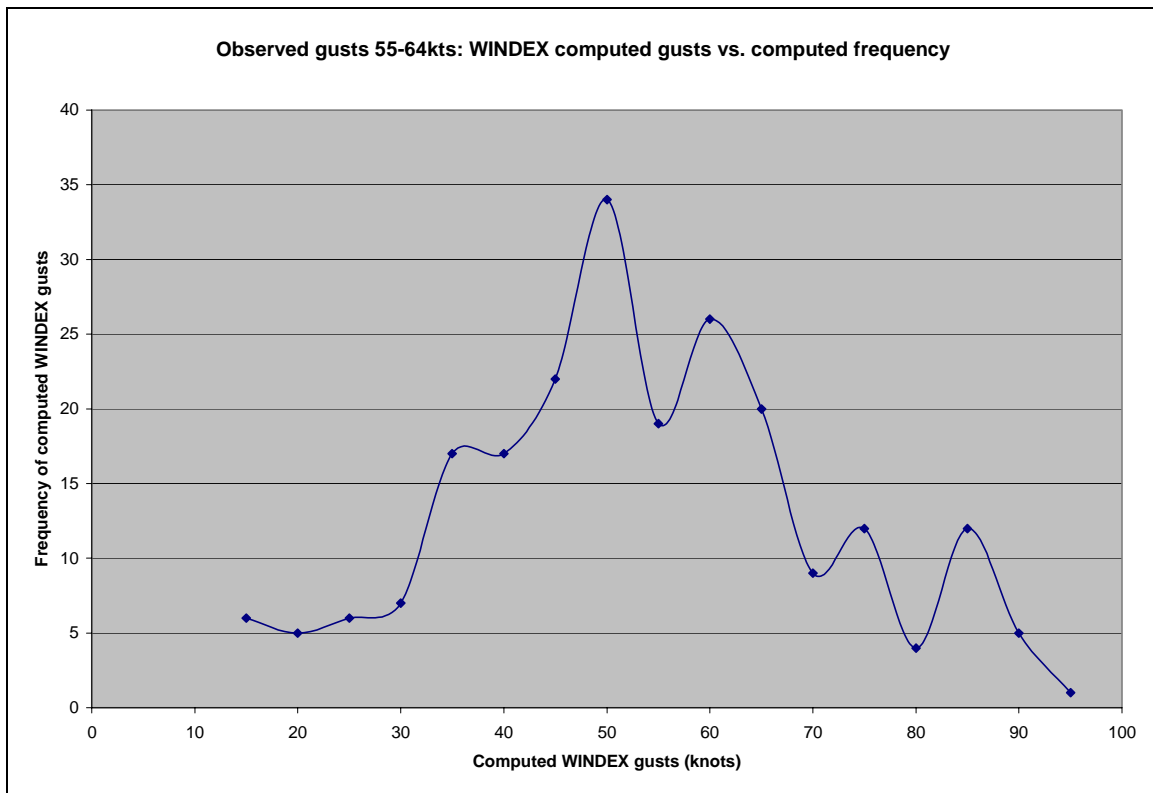
**Figure 4.12.** For observed reports between 35-44 knots: Computed WINDEX wind gusts are compared to the frequency of times it was computed within the range of observed gusts.

Figure 4.13 shows the frequency of computed WINDEX gust values for the observed storm reports between 45 and 54 knots. With the larger number of reports in this range, the frequency chart produces a more Gaussian distribution. The highest frequency of computed WINDEX gust values fell between 61 and 65 knots which is too high and indicates the method overestimates wind gusts. The large spread suggests that the method is not very accurate as well. This large spread may be due to the sensitivity of the method to small variations from grid point to grid point.



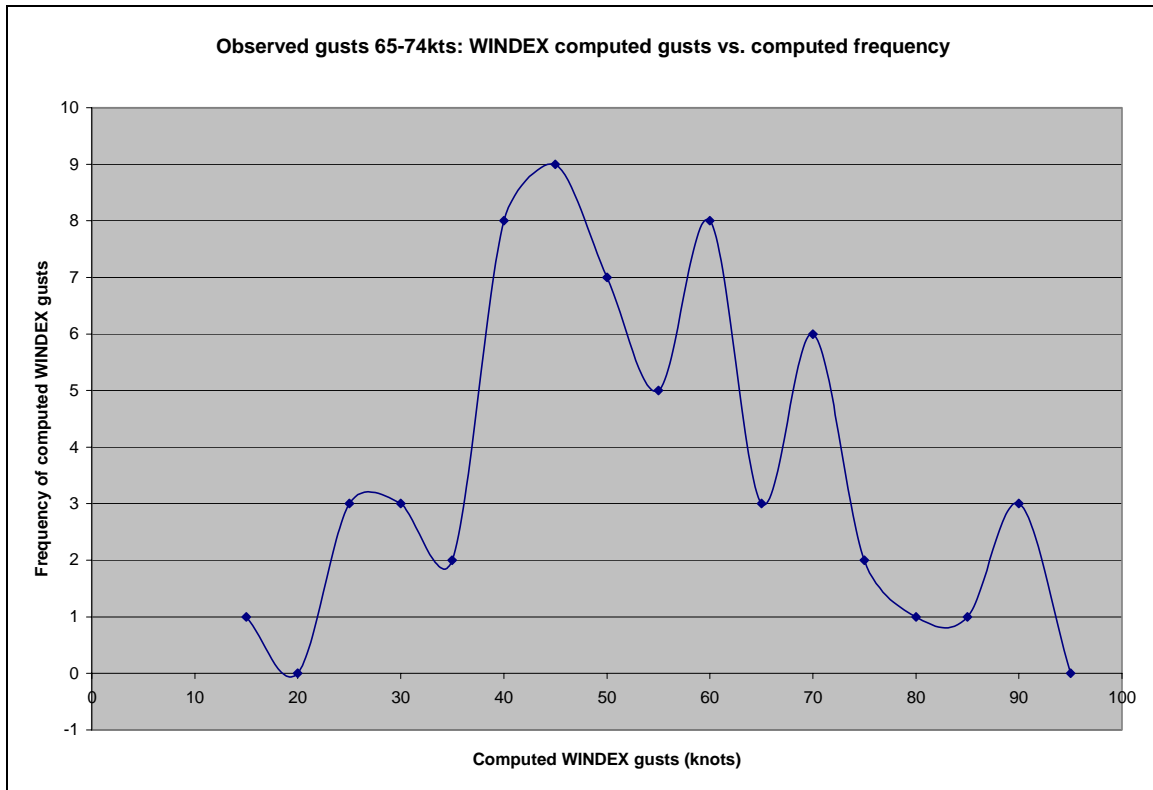
**Figure 4.13.** For observed reports between 45-54 knots: Computed WINDEX wind gusts are compared to the frequency of times it was computed within the range of observed gusts.

Figure 4.14 shows the frequency of computed WINDEX gust values for the observed storm reports between 55 and 64 knots. The highest frequency of computed WINDEX gust values fell between 46 and 50 knots with a second peak between 56 and 60 knots. Surprisingly, the highest frequency now indicates the method tends to underestimate wind gusts for this range although the distribution is skewed toward higher gust values. Again, the broad width of the distribution suggests large uncertainty in the WINDEX prediction.



**Figure 4.14.** For observed reports between 55-64 knots: Computed WINDEX wind gusts are compared to the frequency of times it was computed within the range of observed gusts.

Figure 4.15 shows the frequency of computed WINDEX gust values for the observed storm reports between 65 and 74 knots. The highest frequency of computed WINDEX gust values fell between 41 and 45 knots with a second peak between 56 and 60 knots. As with the previous speed ranges, the highest frequency indicates the method once again underestimated wind gusts for higher observed winds. The broad character of the distribution is also evident for these speeds and highlights the uncertainty in the WINDEX predictions. There were only six observed reports between 75 and 90 knot gust range. Due to this small data sample no relevant conclusions from this range can be made.



**Figure 4.15.** For observed reports between 65-74 knots: Computed WINDEX wind gusts are compared to the frequency of times it was computed within the range of observed gusts.

## **B. DIURNAL EFFECTS**

The environmental temperature near the surface varies substantially depending on the time of day. Atmospheric instability is typically at its highest just after maximum solar heating or around 21Z for this region of study. By 06Z, radiational cooling has caused temperatures near the surface to fall causing instability to decrease near the surface often resulting in a temperature inversion below 5000 feet. Atmospheric instability may still be high enough above the temperature inversion to allow for nocturnal thunderstorms to exist. Nocturnal thunderstorms can create problems for convective wind forecasting methods due to the modified temperature structure near the surface and is examined in the following section.

### **1. $T_1$ Gust Method**

The method for computing  $T_1$  tries to account for nocturnal cooling by incorporating an inversion into the procedure. If the top of the inversion is within 150 mb to 200 mb of the surface, the warmest part of the inversion is used instead of the forecast maximum surface temperature. Accounting for the inversion allows the  $T_1$  method to be more accurate estimating wind gusts during the nighttime hours. Figure 4.16 is a scatter plot of observed wind gusts and computed  $T_1$  values for 21Z during June 2005 representing daytime thunderstorm events. Figure 4.17 is a plot for 06Z representing nighttime thunderstorm events. Comparing the two plots, the 06Z does have slightly lower values than the 21Z plot, but overall the  $T_1$  values do not show much change between daytime events and nighttime events.

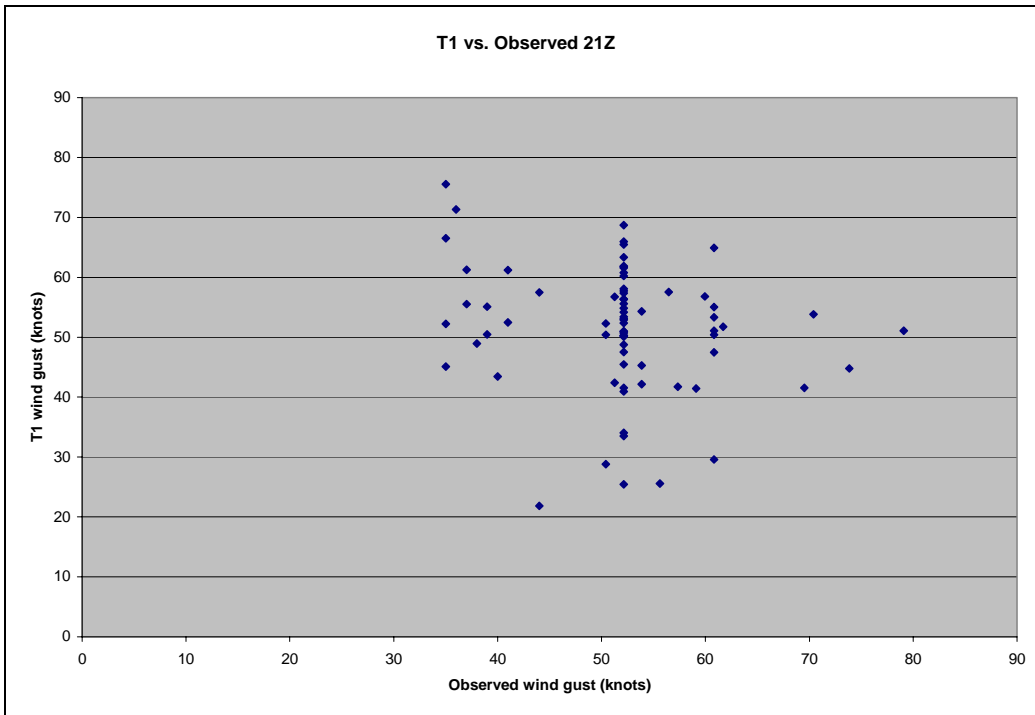


**Figure 4.16.** Computed  $T_1$  gust value versus observed wind gusts for 21Z events during June 2005.

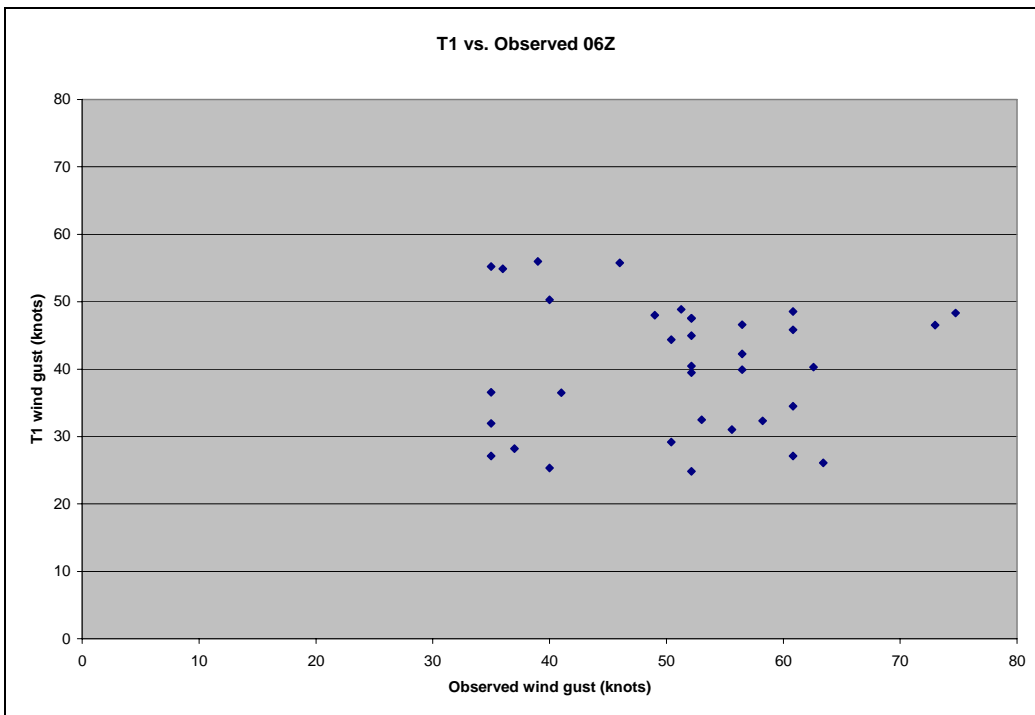


**Figure 4.17.** Computed  $T_1$  gust value versus observed wind gusts for 06Z events during June 2005.

## 2. T<sub>2</sub> Gust Method

The T<sub>2</sub> method computes a value by subtracting the moist adiabat temperature at the surface from the surface dry-bulb temperature then using Figure 2.1 to obtain a gust value. During the daytime hours when surface temperatures are highest, the procedure of using the surface temperature is reasonable. However, using a surface temperature during the nighttime hours will dramatically change the results because the surface temperature is not a true representation of the lower part of the atmosphere due to nocturnal cooling. In addition, the cool surface temperature does not adequately represent the deeper (freezing level to surface) layer of negative buoyancy. Figure 4.18 is a scatter plot of observed wind gusts and computed T<sub>2</sub> values for 21Z during June 2005 representing daytime thunderstorm events. Figure 4.19 is a plot for 06Z representing nighttime thunderstorm events. Both time periods do have low overall T<sub>2</sub> values but the computed gusts for the nighttime events are extremely low with many near zero. The extremely low gusts for the nighttime events show that the T<sub>2</sub> method does not perform well after sunset.

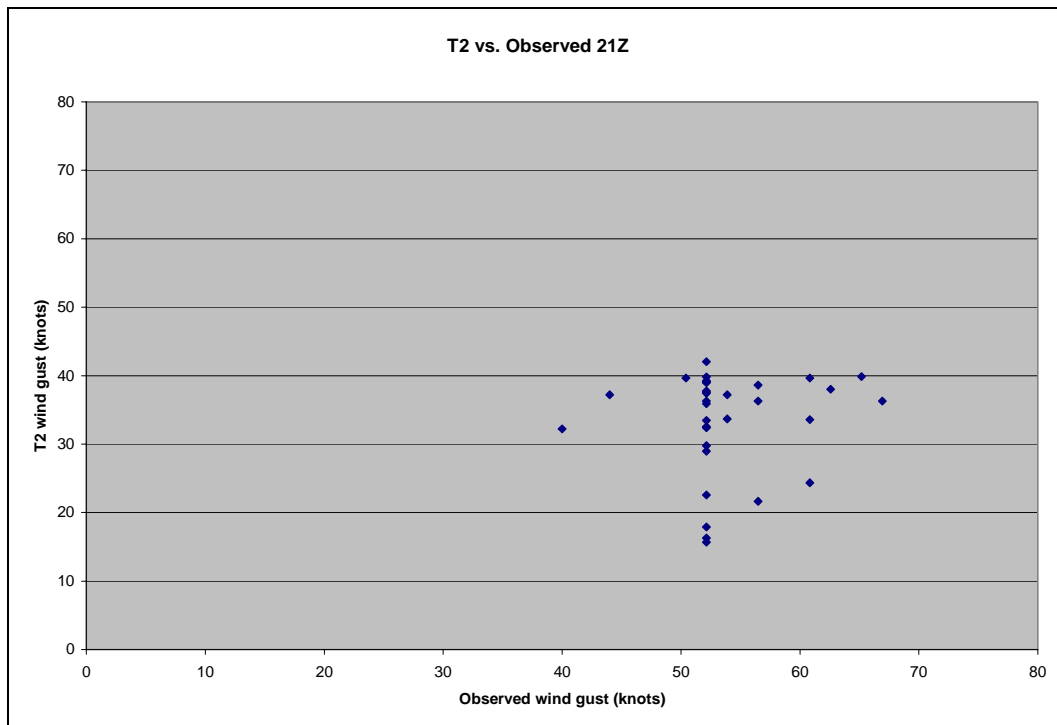


**Figure 4.18.** Computed T<sub>2</sub> gust value versus observed wind gusts for 21Z events during June 2005.



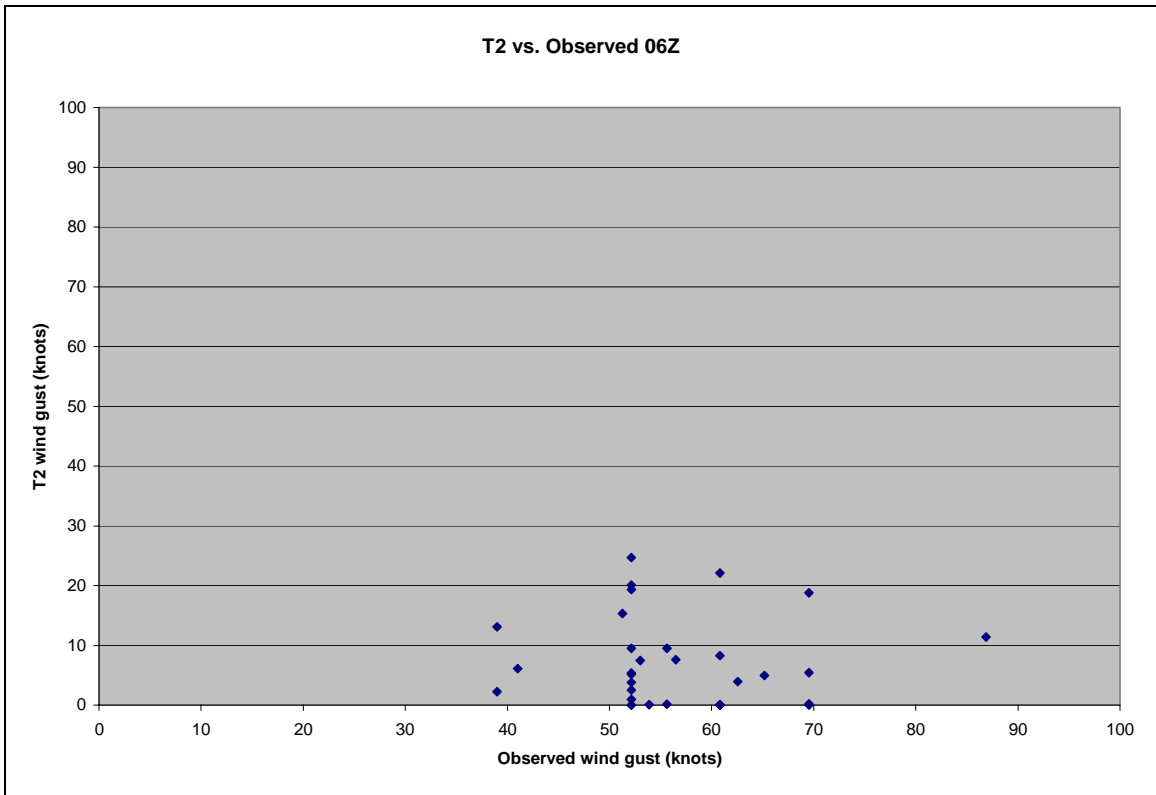


**Figure 4.19.** Computed  $T_2$  gust value versus observed wind gusts for 06Z events during June 2005.

### **3. WINDEX Gust Method**

The method for computing WINDEX uses the average environmental temperature lapse rate between the surface and the melting level. During the daytime hours when the surface temperature is typically warmer, the lapse rate is larger thus providing a good estimated wind gust value using the WINDEX equation. However, during the nighttime hours when surface temperatures are low, the average lapse rate decreases if the surface temperature is used in the calculation. To overcome this limitation of using surface temperature to get the lapse rate, the calculation made in this study used the warmest low level temperature (below 850 mb) to represent the average lapse rate in the deeper atmosphere. Figure 4.20 is a scatter plot of observed wind gusts and computed WINDEX values for 21Z during June 2005 representing daytime thunderstorm events. Figure 4.21 is a plot for 06Z representing nighttime thunderstorm events. WINDEX gusts for the nighttime events show a definite decrease in gust value with many values below 40 knots, while the daytime events are mainly above 40 knots. However, the difference is not as large as that found in  $T_2$ , which supports the use of the warmest temperature in the lowest layer to obtain a more representative lapse rate.

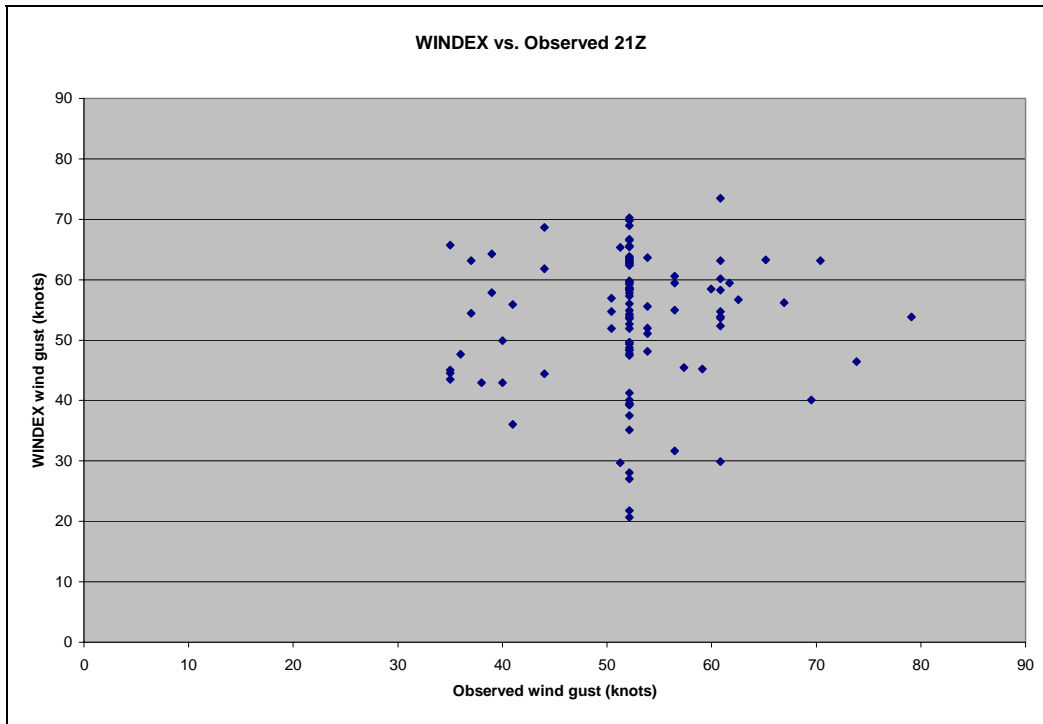


**Figure 4.20.** Computed WINDEX gust value versus observed wind gusts for 21Z events during June 2005.

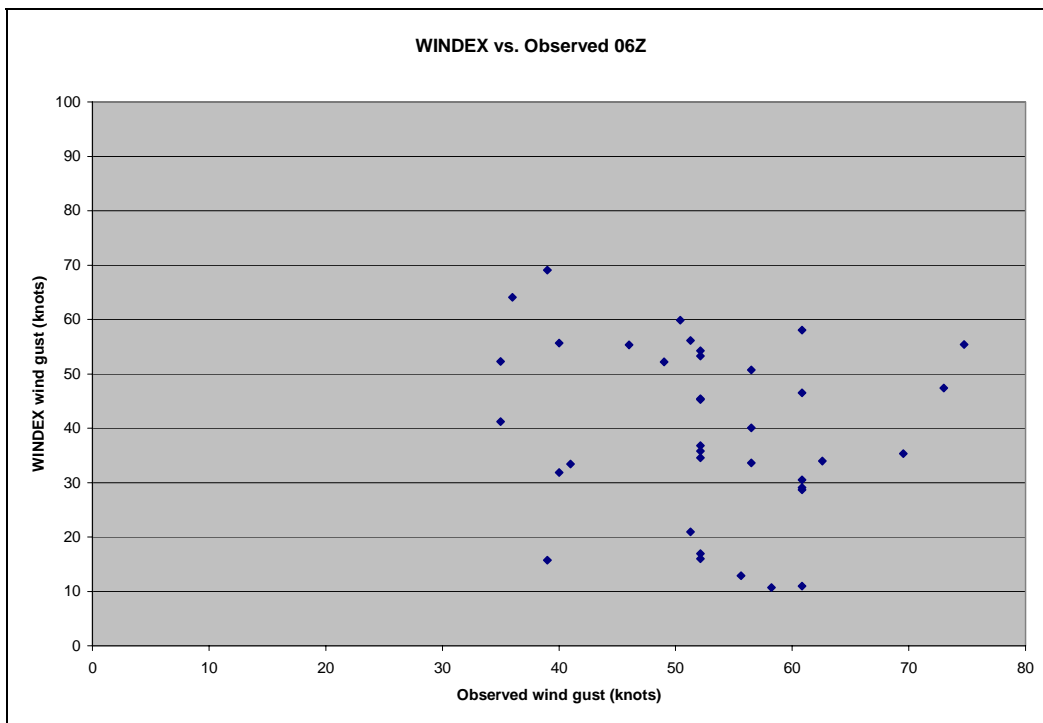
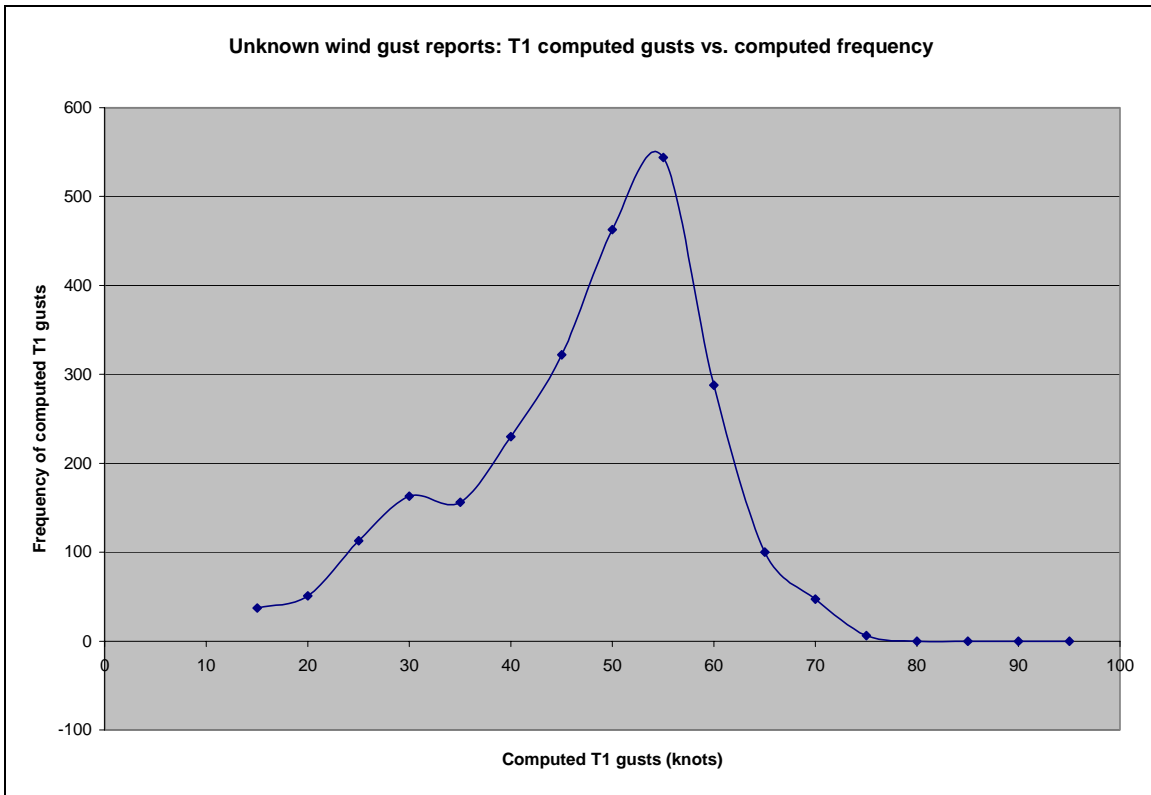


**Figure 4.21.** Computed WINDEX gust value versus observed wind gusts for 06Z events during June 2005.

### **C. REPORTS OF UNKNOWN WIND SPEED**

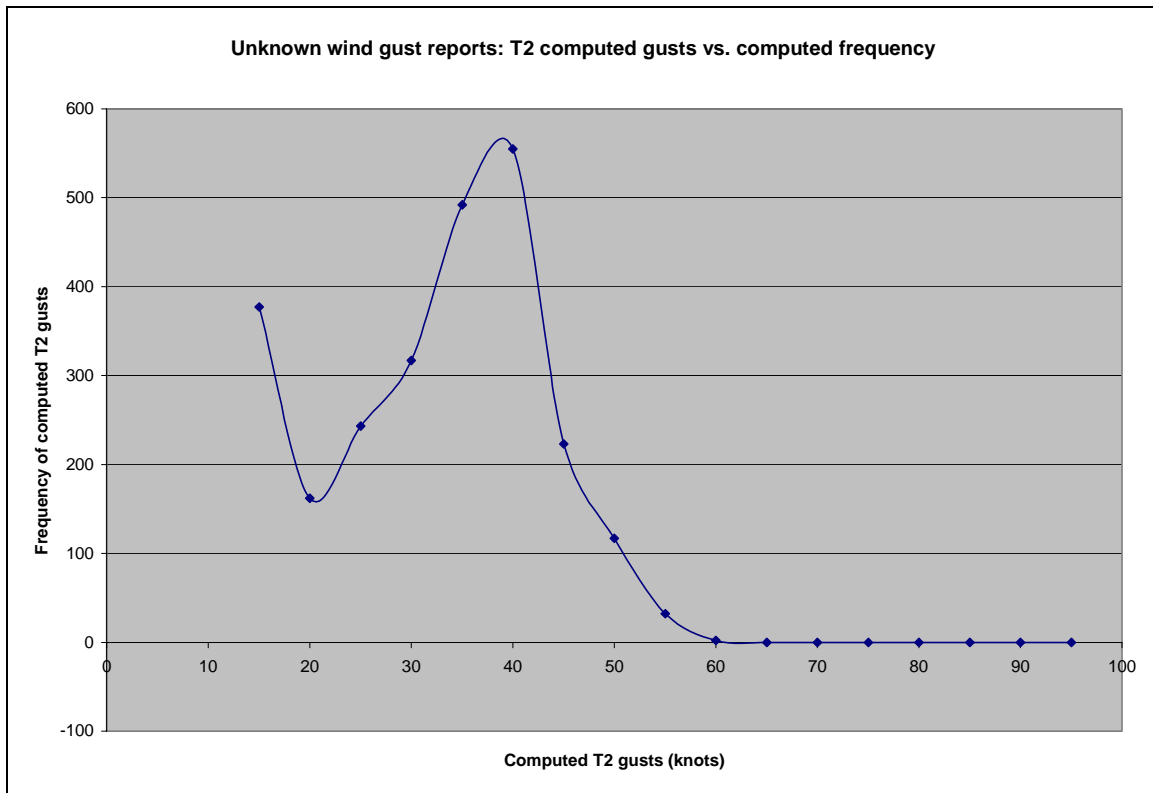
During the months of June and July 2005, there were 2520 severe storm reports where a good estimate of the actual wind gust is unknown. Storm reports are often reported as an unknown wind gust due to the lack of observational equipment and trained severe weather spotters. These reports may not have a wind gust, but information can be extracted by computing wind gust values for each method at the place and time of the unknown storm report. These reports are presumed to be associated with wind gusts 50 knots or greater because of reported damage to trees or other structures.

In Figure 4.22, a frequency chart of the computed  $T_1$  gust values divided into ranges of: less than 15 knots, 15 to 20 knots, 21 to 25 knots, and so on up to 90 knots in 5 knot increments is shown. The highest frequency of values fell between 51 and 55 knots with high frequencies down to 40 knots. The mean  $T_1$  gust value for the 2520 unknown reports was calculated to be 45 knots. Using the mean value, the method slightly underestimated wind gusts assuming that each unknown report resulted from gusts of 50 knots or greater. This underestimate is also suggested by the skewed nature of the distribution in Figure 4.22 which shows more values below the mean than values above the mean. However, the highest frequency of computed values also suggests the method can often be useful at estimating wind gusts.



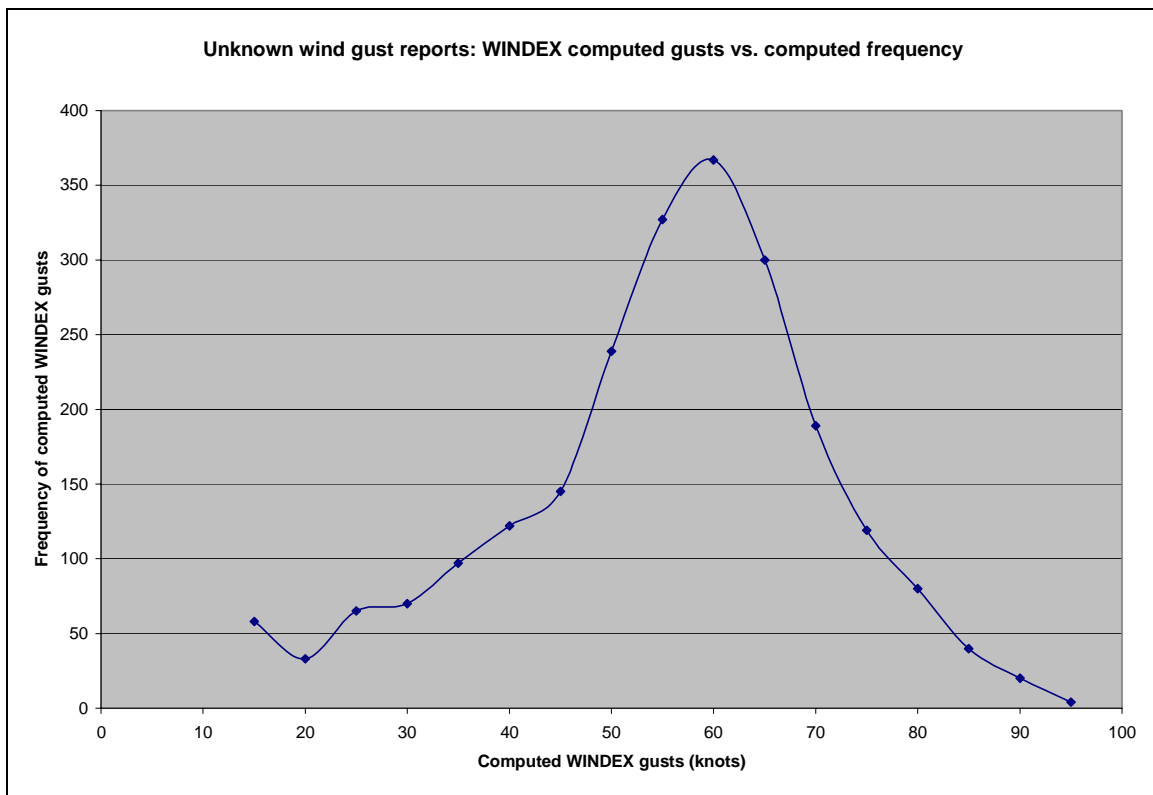
**Figure 4.22.** For unknown wind gusts: Computed  $T_1$  wind gusts are compared to the frequency of times it was computed.

Figure 4.23 shows the frequency of computed  $T_2$  gust values within each range for 2520 reports with unknown wind speeds. The highest frequency of values fell between 41 and 45 knots with high frequencies down to 30 knots. The mean  $T_2$  gust value for the unknown reports was calculated to be only 29 knots due to the high number of low forecasted values during suspected nighttime events. The mean value is very low assuming the storm reports had wind speeds greater than 50 knots. The method's difficulty with handling nighttime events is likely a great contributor why the mean is so low. Given that the distribution is mostly due to warm period (daytime) events, the peak frequency of 41 to 45 knots is still low but suggests that  $T_2$  may be useable under proper conditions.



**Figure 4.23.** For unknown wind gusts: Computed  $T_2$  wind gusts are compared to the frequency of times it was computed.

Figure 4.24 shows the frequency of computed WINDEX gust values within each range for 2274 reports with unknown wind speeds. Reports where the calculated WINDEX value was close to zero were omitted due to the WINDEX equation resulting in values of zero when the environmental lapse rate is less than  $5.5^{\circ}\text{C km}^{-1}$ . The highest frequency of values fell between 56 and 60 knots with high frequencies between 50 and 70 knots. The mean WINDEX gust value for the unknown reports was calculated to be 53 knots because of the tail in the distribution on the low side. The frequency of computed wind gust values and the mean value shows the WINDEX method is a fairly accurate estimate of wind gusts. The distribution for WINDEX is more Gaussian than for  $T_1$  even with its tail on the low end. This suggests a more reliable estimation of wind gusts than  $T_1$ , although the broader spread produces more uncertainty in the estimate.



**Figure 4.24.** For unknown wind gusts: Computed WINDEX wind gusts are compared to the frequency of times it was computed.

#### **D. WIND METHOD COMPARISON**

Convective wind forecasting is complex due to the variability in atmospheric conditions and the inability of correctly predicting these conditions through computer models. If a computer model such as the AFWA MM5 is not accurate in the low levels of the atmosphere, then it is impossible to predict with any accuracy what the potential winds gusts are from a thunderstorm that has yet to form or move over the forecast location. There are also doubts in the accuracy of the reported storm reports. Many of the wind speeds from storm reports are estimated values and sometimes by a non-trained observer. Disregarding the possibility of errors in the observed wind values and model data, the  $T_1$ ,  $T_2$ , and WINDEX methods have been compared to the observed wind gusts to find a percentage difference between the computed method value and the observed value.

Table 4.1 displays percentage differences for all three methods given every three hours for storm reports during June 2005 while Table 4.2 displays the same data for July 2005. A percentage difference was computed by taking the difference between the wind method computed value and the observed value, then dividing the difference by the observed wind gust and multiplying by 100. For example, a wind gust of 50 knots and estimated WINDEX gust of 60 knots results in a percentage difference of 20 percent. The percentage difference computed for all storm reports during the month for each method is also shown.

The percentage difference for the  $T_1$  method was on average 23 percent from the observed wind gusts during June and 21 percent during July. The  $T_2$  method was typically between 35 to 40 percent off during daytime events, but was dramatically higher during nighttime events. WINDEX forecasts were on average 27 percent off observed wind gusts during June and 30 percent during July. All three methods showed the highest accuracy between 18Z to 03Z which correlates with daytime thunderstorm events, while nighttime events showed degraded accuracy.



**Table 4.1.** Percentage difference between the method computed wind gusts and observed gusts for each three hour time frame for June 2005.

<b>Time (UTC)</b>	<b>T<sub>1</sub> Method</b>	<b>T<sub>2</sub> Method</b>	<b>WINDEX Method</b>	<b>Total Reports</b>
00Z	21	43	26	141
03Z	22	59	29	142
06Z	29	88	38	70
09Z	30	89	30	26
12Z	54	69	52	8
15Z	23	68	48	16
18Z	21	35	23	52
21Z	23	37	20	109
<b>All reports</b>	23	57	27	564

**Table 4.2.** Percentage difference between the method computed wind gusts and observed gusts for each three hour time frame for July 2005.

<b>Time (UTC)</b>	<b>T<sub>1</sub> Method</b>	<b>T<sub>2</sub> Method</b>	<b>WINDEX Method</b>	<b>Total Reports</b>
00Z	25	30	36	93
03Z	19	53	24	111
06Z	21	66	32	69
09Z	26	83	24	16
12Z	29	78	52	8
15Z	25	58	32	13
18Z	18	37	24	16
21Z	16	33	29	51
<b>All reports</b>	21	51	30	377

Table 4.3 displays the mean computed wind gust value for five observed gust ranges, while Table 4.4 displays the average one standard deviation from the mean for each forecast method.

**Table 4.3.** Computed forecast mean values in knots for each method for given observed gust ranges.

	<b>35-44 kts</b>	<b>45-54 kts</b>	<b>55-64 kts</b>	<b>65-74 kts</b>	<b>75-90 kts</b>
<b>T<sub>1</sub></b>	48	51	49	50	55
<b>T<sub>2</sub></b>	23	25	27	23	27
<b>WINDEX</b>	49	52	51	50	65

**Table 4.4.** One standard deviation values in knots for each method for given observed gust ranges.

	<b>35-44 kts</b>	<b>45-54 kts</b>	<b>55-64 kts</b>	<b>65-74 kts</b>	<b>75-90 kts</b>
<b>T<sub>1</sub></b>	14	12	12	13	6
<b>T<sub>2</sub></b>	14	14	14	13	15
<b>WINDEX</b>	16	17	18	17	17

## **E. DISCUSSION OF RESULTS**

The data analyzed in this chapter gives insight into the potential benefits and problems of using model-derived wind gusts to predict actual observed convective wind gusts from T<sub>1</sub>, T<sub>2</sub>, and WINDEX methods. Potential data set errors exist due to the likelihood that many observed wind gusts are estimated and only a small amount of reports occur during the nighttime hours. These observational limitations contribute to the uncertainty and variability in the verification of the model forecasts of gusts. The model predicted value may be appropriately representative but not verify very well because the observed gust is estimated. The range of observational uncertainty is potentially as large as the spread in the forecast values and limits the ability to separate predicted gusts

into 10 knot ranges. This is evident in the unknown gust plots in Figures 4.22, 4.23, and 4.24.

The variability in the forecasted wind gusts for a given method can be high due to the sensitivity of the methods' calculation procedure to small variations in the model. As shown previously, Figure 4.1 shows the total observed gusts versus the calculated  $T_1$  gusts, while Figure 4.11 shows the total observed gusts versus the calculated WINDEX gusts. The variability in  $T_1$  gusts lies between 20 to 70 knots which is far less than the variability in the WINDEX gusts that lie between 10 and 90 knots. This is due to the tendency of the  $T_1$  calculation to be insensitive to small changes in environmental conditions. The great deal of variability in the WINDEX gusts is likely due to the high sensitivity of the components of the WINDEX equation to small variations in environmental conditions. This shows that the  $T_1$  gusts are quite often somewhat close to the observed gust, but will often miss important environmental details due to the insensitive nature of the calculation. The WINDEX gust estimates may be very accurate for some observed gusts, but due to the higher sensitivity to mesoscale features in the method's calculation, the WINDEX values are subject to greater variability in the forecasted gust values than is  $T_1$ .

The constructed frequency plots in this chapter for  $T_1$  and WINDEX are encouraging in some aspects. The plots show a good Gaussian nature to the distributions for the different observed gust range; however, the curves are far from a perfect Gaussian distribution as the model-derived gust spread is too high. The plots for each method utilizing the unknown wind speed reports are even more Gaussian in nature compared to the frequency plots. This suggests that over a larger data set, the wind methods can be a useful estimate for determining potential thunderstorm wind gusts.

The  $T_2$  gust estimates were greatly erroneous for the majority of the data set. This is mainly due to the nighttime events when the  $T_2$  calculation is skewed due to the use of the model-derived surface temperature at the time of the observed gust instead of the previous maximum temperature during the daytime.

Even if only daytime events are analyzed using the  $T_2$  method, there is still a large underestimate for most observed wind gusts. This is likely due to the calculation procedure in  $T_2$  not utilizing the entire column from the wet-bulb zero height to the surface when considering the amount of energy that goes into determining downdrafts. Negative buoyancy might occur through the entire column but vanish at the lowest level. This yields a near zero  $T_2$  gust estimate but completely misses the downdraft potential above. This could be addressed through a modified calculation procedure.

Overall, the  $T_1$  method was the most accurate for this study and was less susceptible to varying environmental conditions. All three convective wind gust methods were more accurate during the daytime hours with  $T_2$  performing very poorly during non-daytime hour events. The  $T_1$  method tends to overestimate wind gusts for observed wind speeds of less than 55 knots and underestimate for observed wind speeds greater than 55 knots. The  $T_2$  method consistently underestimated wind gusts for all events, even during the daytime events. The WINDEX method was found to be the most sensitive of the three methods, and nearly as accurate as  $T_1$  overall. WINDEX did tend to overestimate wind gusts for most observed wind speed ranges; however, performed better than the other methods on observed wind speeds greater than 65 knots.

## **V. CONCLUSIONS AND RECOMMENDATIONS**

### **A. CONCLUSIONS**

Based on this study, there is lots of uncertainty in the  $T_1$ ,  $T_2$ , and WINDEX methods. The  $T_1$  and  $T_2$  methods are limited by their insensitivity to variability in atmospheric structure due to the simplistic nature of the calculations, while WINDEX is much more sensitive to varying environmental conditions. Probable errors in the dataset because the observed wind gusts are often estimated rather than accurately measured, pose a problem in accessing the accuracy of the model data. While the model computed gusts may be questionable, there is useful guidance given by the model-derived wind gusts. The model forecasts provide consistent spatial predictions of the convective wind gust methods and can be applied over a region to estimate potential high wind gust areas wherever a thunderstorm may occur.

The  $T_1$  method is the more stable estimate than WINDEX due to  $T_1$  not relying on model fields like moisture that are generally more poorly forecast. WINDEX is more sensitive to problems in the model fields due to its more complex calculation, but can also predict extreme gusts from the model data. If WINDEX were properly calibrated for known model biases or consistent errors, it would likely be a consistent indicator of potential wind gusts. Overall, the  $T_1$  and WINDEX methods suggest some potential for model-derived gust forecasts to be made. While encouraging, the results from this study show that the ability of even short-term (less than 12 hours) forecasts to capture the complete atmospheric structure that leads to convective gusts of a given speed is difficult at best. The best use of the model-derived guidance might be to treat any model forecasts of gusts above something like 40 knots as indicative of the potential for gusts of some destructive magnitude.

### **B. RECOMMENDATIONS**

As a result of the study, the following recommendations for further research are suggested:

- A broader data set should be used. For instance, a data set that encompassed an entire years worth of wind events would give a better sampling than two months.
- Compare the AFWA MM5 algorithm for model-derived  $T_1$  and  $T_2$  wind speeds to those calculated in this study to ensure proper application to MM5 data.
- Fine tune the wind gust method procedures for the model based on known model biases. This would definitely improve the reliability of the calculations
- Concentrate the study over a much smaller region with more accurate and many more observation locations over a period of few years to get the best possible data set.

## LIST OF REFERENCES

- 15<sup>th</sup> Operational Weather Squadron, Scott AFB, IL, cited February 2006: 15<sup>th</sup> OWS AOR.
- Air Force Weather Agency, Offutt AFB, NE, 2005: AFWA Technical Notes-98/002 Revised: Meteorological Techniques. *Air Force Weather Agency*, 3-26 – 3-28.
- Fawbush, Ernest J. and Miller, Robert C., 1954: A Basis for Forecasting Peak Wind Gusts in Non-Frontal Thunderstorms. *Bulletin American Meteorological Society*, **35**, 14-19.
- Kelly, Donald L., Schaefer, Joseph T., and Doswell, Charles A. III, 1985: Climatology of Nontornadic Severe Thunderstorm Events in the United States. *Monthly Weather Review*, **113**, 1997-2014.
- McCann, Donald W., 1994: WINDEX-A New Index for Forecasting Microburst Potential. *Weather and Forecasting*, **9**, 532-541.
- Miller, Robert C., 1972: Notes on Analysis and Severe-storm Forecasting Procedures of the Air Force Global Weather Central. *Air Weather Service: Technical Report 200 (Rev)*, 10-1 – 10-5.
- National Climatic Data Center, cited February 2006: NEXRAD National Mosaic Reflectivity Images. [Available online at <http://www4.ncdc.noaa.gov/cgi-win/wwwcgi.dll?WWNEXRAD~Images2>].
- NWS Storm Prediction Center, cited February 2006: Index of Severe Thunderstorm Events. [Available online at <http://www.spc.noaa.gov/climo/>].
- Proctor, Fred H., 1988: Numerical Simulations of an Isolated Microburst. Part I: Dynamics and Structure. *Journal of the Atmospheric Sciences*, **45**, 3137-3160.
- , 1989: Numerical Simulations of an Isolated Microburst. Part II: Sensitivity Experiments. *Journal of the Atmospheric Sciences*, **46**, 2143-2165.
- Srivastava, R. C., 1985: A Simple Model of Evaporatively Driven Downdraft: Application to Microburst Downdraft. *Journal of Atmospheric Sciences*, **42**, 1004-1023.
- , 1987: A Model of Intense Downdrafts Driven by the Melting and Evaporation of Precipitation. *Journal of Atmospheric Sciences*, **44**, 1752-1773.

University Corporation for Atmospheric Research, cited February 2006:  
Operational Models Matrix: Characteristics of Operational NWP Models.  
[Available online at <http://meted.ucar.edu/nwp/pcu2/index.htm>]

Wakimoto, Roger M., 2001: Convectively Driven High Wind Events. *Severe Convective Storms: American Meteorological Society*, **28**, 255-298.



## INITIAL DISTRIBUTION LIST

1. Defense Technical Information Center  
Ft. Belvoir, Virginia
2. Dudley Knox Library  
Naval Postgraduate School  
Monterey, California
3. 15<sup>th</sup> Operational Weather Squadron  
Scott Air Force Base, Illinois
4. Wendell A. Nuss  
Monterey, California
5. Carlyle H. Wash  
Monterey, California
6. Department of Meteorology  
Naval Postgraduate School  
Monterey, California
7. Christopher J. Kuhlman  
Keesler Air Force Base, Mississippi